Int Journ Earth Sciences (1999) 88:551–570 © Springer-Verlag 1999

ORIGINAL PAPER

T. Steuber

Isotopic and chemical intra-shell variations in low-Mg calcite of rudist bivalves (Mollusca-Hippuritacea): disequilibrium fractionations and late Cretaceous seasonality

Received: 12 February 1998 / Accepted: 24 May 1999

Abstract Isotopic ($\delta^{13}C$, $\delta^{18}O$) and elemental (Mg, Sr, Mn, Fe) compositions were analysed in sclerochronological profiles of several shells of late Cretaceous rudist bivalves from Greece, Turkey, Somalia and the Arabian Peninsula. The preservation of original compositions of low-Mg calcite of outer shell layers is indicated by constant and high Sr, generally low Fe and Mn, and the preservation of fibrous-prismatic ultrastructures. Cyclic variations in $\delta^{18}O$ and Mg are interpreted to reflect seasonal temperature/salinity cycles and, thus, annual growth increments. In shells of *Torreites*, amplitudes of correlated $\delta^{13}C$ and $\delta^{18}O$ cycles cannot be related to reasonable palaeotemperatures or salinity. This isotopic pattern reflects vital fractionations of an extent which is unknown from modern bivalves. In contrast, almost identical ranges and amplitudes of $\delta^{18}O$ cycles are observed in 13 shells of five species from Santonian-Campanian localities in central Greece and northern Turkey, suggesting that seasonal variations in environmental conditions were recorded without significant vital fractionations. The effect of seasonal salinity changes on $\delta^{18}O$ of the shells is evaluated, and mean palaeotemperatures are constrained within the range of 30–32.5 °C. The annual range of temperature was estimated to be 7 °C, assuming a constant salinity. This agrees with other isotopic proxies of Late Cretaceous palaeotemperatures, and with global circulation models which predict higher low-latitude sea-surface temperatures than the present ones.

T. Steuber
Institut für Geologie und Mineralogie,
Universität Erlangen-Nürnberg, Schlossgarten 5,
D-91054 Erlangen, Germany
e-mail: steuber@geol.uni-erlangen.de
Tel.: +9131-8522514
Fax: +9131-8529295

Key words Rudist bivalves · Cretaceous · Stable isotopes · Sclerochronology · Palaeotemperatures

Introduction

During the Cretaceous, rudist bivalves evolved to be among the most important bioconstructors and carbonate producers in shallow marine tropical and subtropical environments (Ross and Skelton 1993). Rudist associations are generally bound to normal marine environments (Philip 1972). There are a few examples for tolerance against significant salinity changes, but the distribution of rudists in hyper- or mixohaline environments is scarce (Gili et al. 1995).

Rudist shells are composed of an outer calcite and inner aragonite layers (Kennedy and Taylor 1968; Skelton 1974). The inner, aragonitic shell layers have been almost generally converted to low-Mg calcite (LMC). The preservation of the outer layer is usually better, because it originally consisted of diagenetically more stable, fibrous prismatic low-Mg calcite (Al-Aasm and Veizer 1986a, 1986b). The large size and the thick outer shell of late Cretaceous rudist bivalves promises a high temporal resolution of sampling for analysis of chemical and isotopic compositions in sclerochronological profiles. Studies of structural (Pannella and MacClintock 1968; Rhoads and Lutz 1980), elemental (Rosenberg and Hughes 1991; Klein et al. 1996a, 1996b) and isotopic (Mook 1971; Jones et al. 1984; Wefer and Berger 1991) compositions of modern bivalves have shown that environmental changes are recorded to a large extent. In rudist shells, cyclic variations in oxygen isotopic compositions have been interpreted to reflect seasonal variations in palaeotemperature and/or salinity (Steuber 1996a) and, thus, allowed for the quantification of critical aspects of the benthic communities of Cretaceous carbonate platforms such as skeletal growth rates and carbonate production (Steuber 1997; Steuber et al. 1998).

In the present paper, the geochemical data obtained from several species from various late Cretaceous Tethyan environments are summarized, and their potential and limits as proxies of still controversially debated Cretaceous palaeoclimates are evaluated.

Materials

Shells were collected form the following localities (Fig. 1):

1. Shells of the hippuritid *Vaccinites cornuvaccinum* (Bronn) were obtained from life position from Santonian–early Campanian impure limestones of Beotia, central Greece (Steuber 1996b, 1997). Microfacies analysis of the embedding sediment indicate a protected, lagoonal environment. From the same depositional system is a single valve of the radiolitid *Gorjanovicia* cf. *costata* (Polšak) that lived on the more turbulent seaward slope of a rudist bank (Steuber 1996a).
2. A large number of specimens were collected from life position from early Campanian deposits near Amasya village, northern Turkey. Several species shared a turbulent, mixed calcareous-siliciclastic environment at the southern slope of the late Cretaceous Pontid magmatic arc (Steuber et al. 1998). Eight shells of three species (*Vaccinites ultimus* (Milovanović), *V. vesiculosus* (Woodward), *Yvaniella alpani* Karacabey) were found to be sufficiently well preserved for geochemical analysis.
3. A single shell of *Vaccinites grossouvrei* (Douvillé) was collected loose from late Turonian-? Coniacian impure limestones of the Ptoon Mountaines (central Greece).
4. A shell of the radiolitid rudist *Durania* aff. *mutabilis* (Stoliczka) is from the basal Simsima Formation (Campanian-Maastrichtian transition) of Jebel Faiyah, United Arab Emirates, and probably lived in an intertidal environment (Skelton et al. 1990).
5. Three shells of *Torreites sanchezi milovanovici* (Grubić) derive from the early Campanian Samhan Formation of central Oman (Schumann 1995).
6. A single specimen of *Vaccinites macgillavryi* (Palmer) was collected from the Campanian Tisjé Formation of northern Somalia (Pons et al. 1992).

The specimens can be attributed to two different palaeogeographical and thus palaeoclimatic settings (Fig. 1). The late Cretaceous palaeolatitude of central Greece and the Pontid magmatic arc was approximately 30 N, whereas specimens from Oman, Saudi Arabia and Somalia lived in palaeo-equatorial latitudes.

Geochemical data that have been presented in other papers which were predominantly concerned with palaeoecological and palaeobiological interpretations (Steuber 1996a, 1996b, 1997; Steuber et al. 1998) are summarized here (Table 1), and previously unpublished data are presented in sclerochronological profiles.

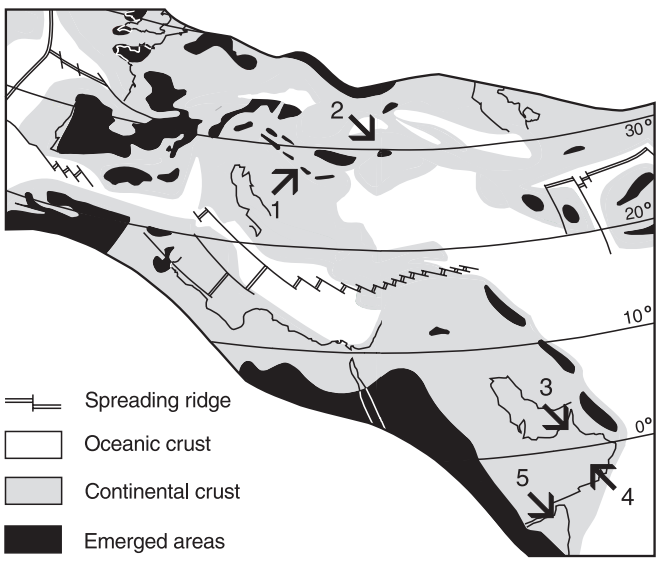


Fig. 1 Palaeogeography of Santonian-Campanian central Tethys (modified from Dercourt et al. 1985). Sampling localities of analysed rudists are indicated by *arrows: 1* central Greece, western Pelagonian margin; *2* northern Turkey, Pontid magmatic arc; *3* United Arab Emirates; *4* central Oman; *5* northern Somalia

Methods

Geochemical analyses were confined to shells in which the fibrous-prismatic ultrastructures are well preserved (Fig. 2). These shells showed distinct growth bands in the outer shell (Fig. 3) when inspected microscopically in longitudinal thick sections (1–1.5 mm).

Sclerochronological profiles for stable isotope analyses were sampled from longitudinal thick sections of right valves with stainless steel burrs (0.5–1 mm ø). Parts of the shells that were recrystallized, cut by fines cracks, or spotted with borings of sponges and other bioeroders were not sampled.

Organic matter within the outer shell layers was found to affect mass spectrometric analyses so that sample powders were heated in vacuo at 180 °C for 5–8 h. Average sample size was 1 mg, and minimum sample size for reaction in off-line preparation lines was 400 μg. Smaller samples have been analysed with an automated on-line device (Finnigan Carbo Kiel). Calcite samples were reacted with H_3PO_4 following standard methods and measured with either Finnigan Delta S, MAT 252, or VG Optima mass spectrometers. All reported δ-values refer to the PDB standard if no other standard is indicated. Reproducibility of isotopic results (± 0.08‰ $\delta^{13}C$ and ± 0.1‰ $\delta^{18}O$) was monitored by continuous analyses of NBS19 and a laboratory standard. Palaeotemperatures (Table 1) were calculated according to Anderson and Arthur (1983):

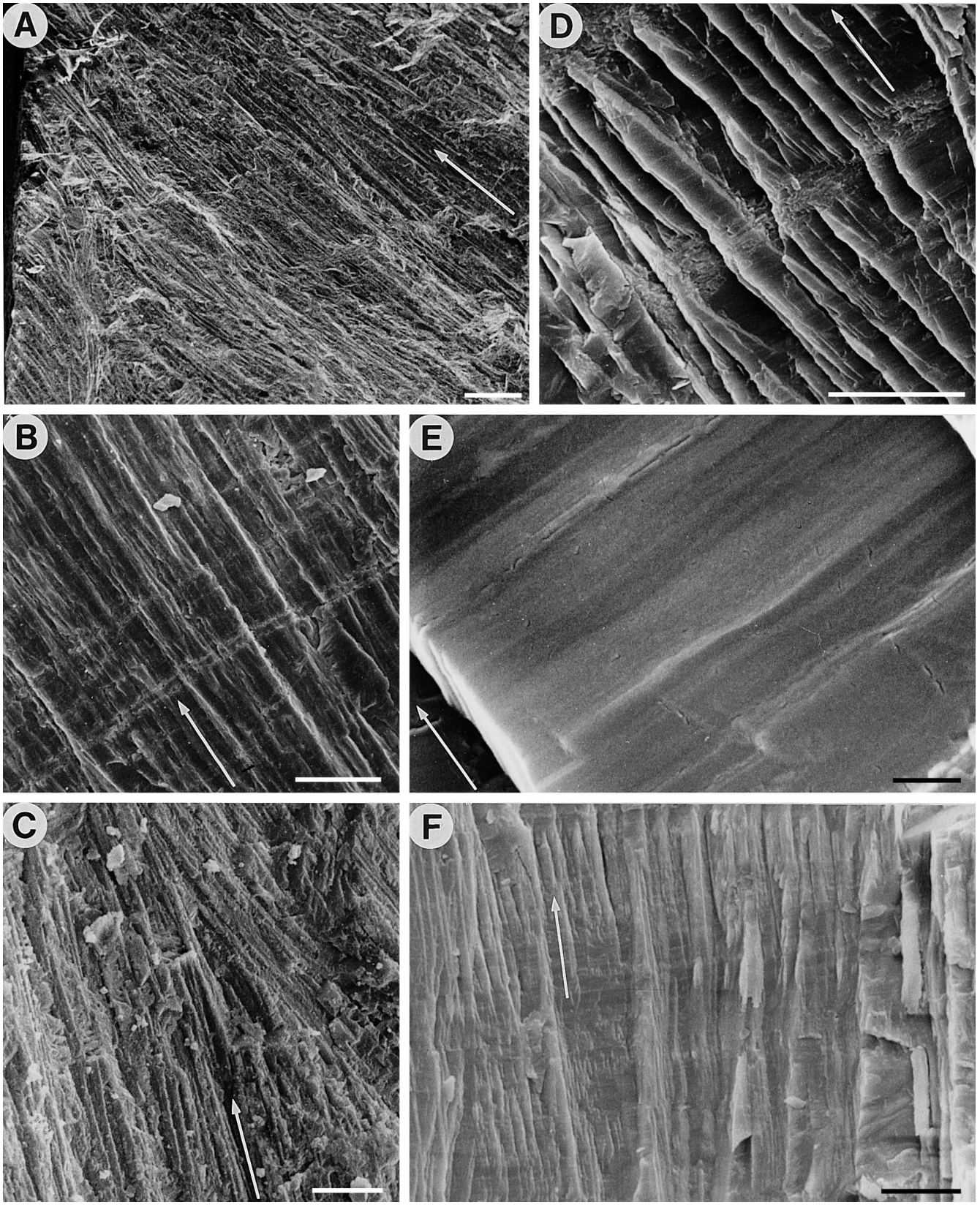


Fig. 2A–F SEM micrographs of radially fractured outer shell layers showing preservation of fibrous prismatic ultrastructure. **A,B** *Vaccinites cornuvaccinum* (H525); C, *V. macgillavryi* (H575); **D–F** *Torreites sanchezi milovanovici* (H576, H579). *Scale bar* is 300 μm (**A**), 30 μm (**B–D, F**) and 1 μm (**E**)



Fig. 3 Longitudinal thick section of *Torreites sanchezi milovanovici* (H576). Chemical and isotopic compositions of this specimen are shown in Fig. 12. Length of shell is 150 mm

$$T[^{\circ}C] = 16.0 - 4.14(\delta CaCO_3 - \delta H_2O[SMOW]) + 0.13(\delta CaCO_3 - \delta H_2O[SMOW])^2$$

Samples for analyses of elemental compositions (Mg, Sr, Mn and Fe) of shell carbonates were drilled with tungsten instruments (ø1 mm) in profiles parallel to those that were sampled for isotopic analyses. Growth banding allowed for the correlation of samples drilled for the analysis of chemical and isotopic compositions. Approximately 1 mg of the sample powder was carefully weighed, dissolved in 1 ml of 1 N HCl, and the solution was then diluted with 4 ml of H_2O and analysed by inductively coupled plasma-atomic emission spectrometry (ICP-AES). Precision of threefold analyses was better than ±2% of the measured concen-

Table 1. Summary of $\delta^{13}C$ and $\delta^{18}O$ analytical results, inferred individual ages, vertical growth rates, and palaeotemperatures, assuming –0.5‰ $\delta^{18}O$ (SMOW) of late Cretaceous seawater

Specimen no.	$\delta^{13}C$ (‰)			$\delta^{18}C$			*r*	*N*	Cycles (years)	Temperature (°C)		
	Min.	Max.	Mean	Min.	Max.	Mean				Min.	Mean	Max.
Beotia, central Greece												
Vaccinites cornuvaccinum												
H479[a]	−0.55	1.78	1.32	−5.14	−3.06	−3.82	+0.60	25	1	27.5	32.3	38.0
H102	1.40	2.48	2.05	−4.71	−3.13	−4.01	+0.53	21	1	27.8	31.8	35.7
H525	0.02	2.15	1.38	−5.21	−3.56	−4.26	+0.26	68	7	29.9	34.2	38.4
H78[b]	0.15	2.82	1.61	−5.25	−2.64	−3.84	+0.23	68	4	25.5	32.1	38.6
Gorjanovicia cf. *costata*												
R561[c]	0.74	2.62	1.83	−4.61	−2.09	−3.35	+0.36	81	2	22.9	29.1	35.2
Vaccinites grossouvrei												
H582	1.97	2.97	2.53	−2.69	−1.37	−2.01	−0.18	62	–	–	–	–
Amasya, northern Turkey												
Vaccinites ultimus												
H589[c]	0.74	1.96	1.40	−5.28	−2.88	−4.14	−0.51	176	2	26.6	32.7	38.8
H587	0.87	2.21	1.73	−4.71	−2.91	−3.88	−0.43	146	4	26.7	31.2	35.7
H588[d]	1.24	2.66	1.86	−4.44	−2.91	−3.74	−0.63	46	2	26.7	30.5	34.3
H584[d]	0.86	2.51	1.88	−5.01	−3.20	−4.10	−0.31	136	4	28.1	32.7	37.3
Yvaniella alpani												
H588[d]	2.17	3.50	2.71	−3.99	−2.84	−3.29	−0.45	29	1	26.4	29.2	32.0
H590[d]	1.74	2.43	2.03	−5.21	−2.95	−3.92	+0.19	37	3	26.9	32.7	38.4
H586[d]	1.76	2.66	2.18	−5.47	−3.17	−4.34	−0.17	74	6	28.0	33.9	39.8
Vaccinites vesiculosus												
H591[d]	1.21	2.32	1.82	−5.12	−2.87	−3.90	+0.35	43	3	26.5	32.2	37.9
Oman												
Torreites sanchezi milovanovici												
H576	−2.00	1.56	−0.09	−7.13	−4.25	−5.75	+0.79	132	(?6)	33.4	41.3	49.2
H579	−2.06	1.55	0.02	−6.80	−4.17	−5.77	+0.77	242	(?6)	32.9	40.1	47.2
H585	−2.16	0.97	−0.05	−6.77	−3.76	−5.36	+0.69	132	?	30.9	39.0	47.1
United Arab Emirates												
Durania aff. *mutabilis*												
R879	−0.24	1.31	0.34	−4.95	−1.43	−2.49	−0.40	96	–	–	–	–
Somalia												
Vaccinites macgillavryi												
H575	−2.73	2.08	0.55	−7.91	−3.34	−5.41	+0.60	137	–	–	–	–

Data which are not figured in this paper are presented as sclerochronological profiles in: [a]Steuber (1996b); [b]Steuber (1997); [c]Steuber (1996a); and [d]Steuber et al. (1998)

trations. A limited precision of weighing reduced the reproducibility to 10% of the analysed concentrations. Detection limits for Fe and Mn at the chosen dilution were 80 and 8 ppm, respectively.

Results

Preservation of original chemical and isotopic compositions

Diagenetic compositional changes of calcareous fossils have been studied extensively (e.g. Brand and Veizer 1980; Veizer 1983; Banner and Hanson 1990), including the effect of diagenesis on the isotopic and elemental composition of aragonite and LMC in rudist shells (Al-Aasm and Veizer 1986a, 1986b; Woo et al. 1992, 1993).

The meteoric diagenesis of LMC typically results in increasing Mn and Fe concentrations, whereas levels of Sr and Mg decrease (Brand and Veizer 1980; Al-Aasm and Veizer 1982). Sr and Mn are generally considered to be particularly indicative of a diagenetic overprint (Veizer 1983). The mean values of both elements in most investigated rudist shells fall into a range of compositions that have been found in calcite shells of extant marine bivalves (Fig. 4; Table 2). Lower Sr and higher Mn concentrations have been measured in several samples of *Vaccinites cornuvaccinum*, *V.*

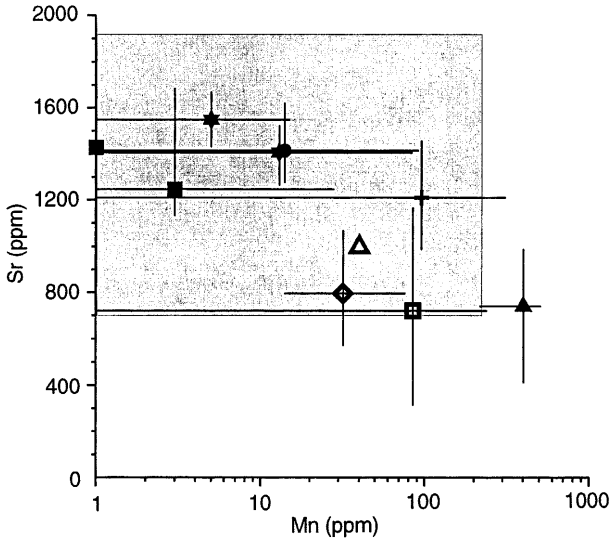


Fig. 4 Ranges and means of Mn and Sr concentrations found in sclerochronological profiles of outer shell layers of *Gorjanovicia* cf. *costata* (*dot*); *Vaccinites cornuvaccinum* (*cross*); two shells of *Vaccinites ultimus* (*stars*); two shells of *Torreites sanchezi milovanovici* (*black boxes*); *Vaccinites grossouvrei* (*diamond*); *Vaccinites macgillavryi* (*white box*); *Durania* aff. *mutabilis* (*black triangle*). *White triangle* is average composition of modern bivalve calcite (compiled by Al-Aasm and Veizer 1986a) and *shaded area* indicates range of concentrations of recent marine bivalve calcite shells (compiled from Vinogradov 1953; Turekian and Armstrong 1960; Leutwein and Waskowiak 1962; Pilkey and Goodell 1963; Hallam and Price 1968; Milliman 1974)

Table 2. Elemental compositions (ppm) of outer shell layers of various Hippuritidae and Radiolitidae. Concentrations below the analytical detection limit of Mn and Fe were considered as zero so that correct mean values could be slightly higher. (r_{13} = correlation coefficient δ^{13}C-Mg; r_{18} = correlation coefficient δ^{18}O-Mg)

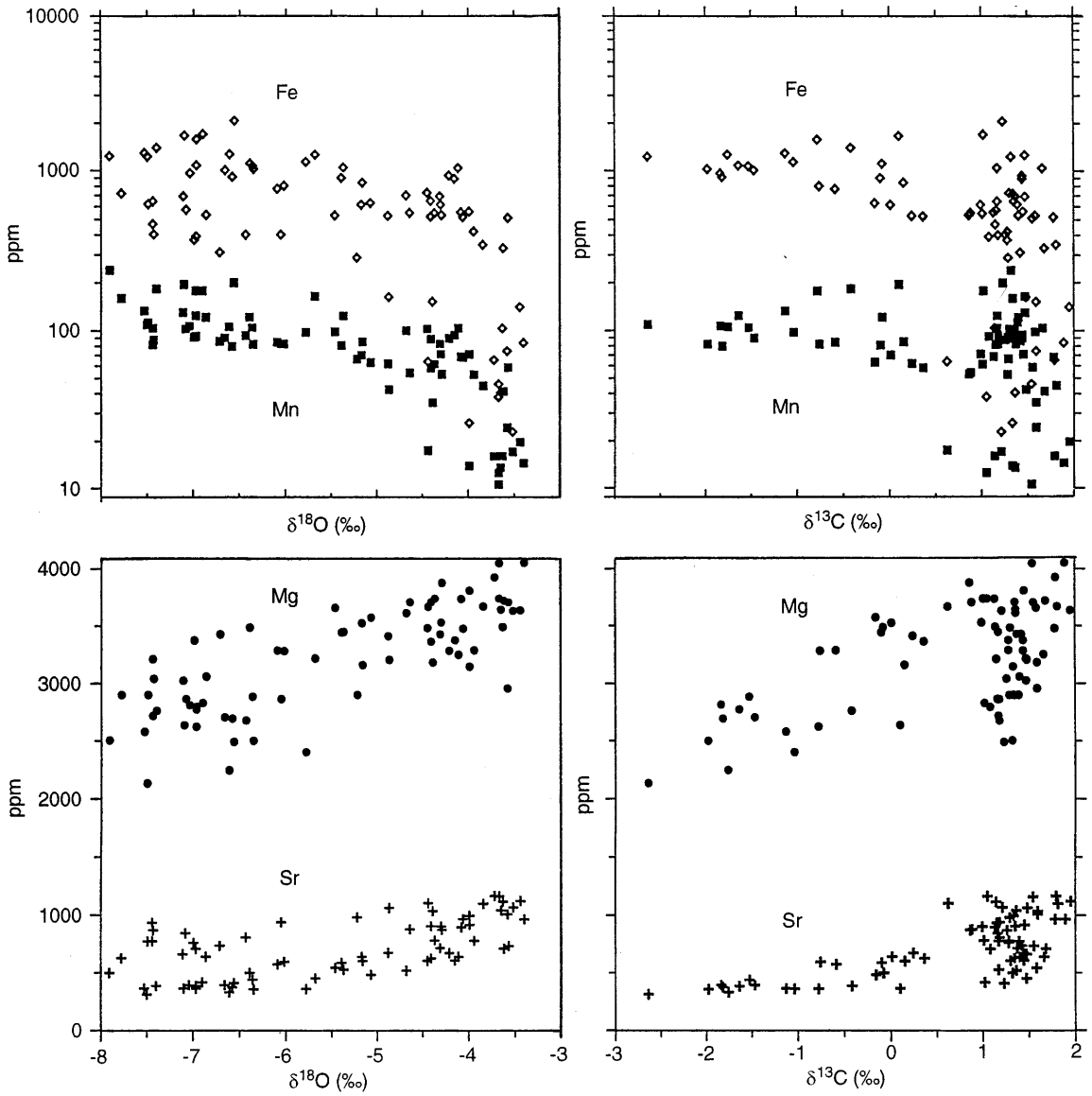
Specimen	*N*	r_{13}	r_{18}		Mg	Sr	Mn	Fe
Vaccinites cornuvaccinum (Bronn) H525	42			Min.	876	987	<8	<80
				Max.	2512	1455	311	908
				Mean	1305	1210	96	81
Gorjanovicia cf. *costata* Polšak R561	24	+0,12	−0.80	Min.	1075	1276	<10	<80
				Max	2191	1621	92	<80
				Mean	1472	1415	14	<80
Vaccinites grossouvrei (Douvillé) H582	68	+0,23	+0,07	Min.	3962	572	14	<80
				Max.	5744	1070	76	1222
				Mean	4808	796	32	205
Vaccinites ultimus (Milovanović) H589	47	+0.47	−0.69	Min.	1453	1430	<8	<80
				Max.	2478	1670	15	2574
				Mean	1939	1549	5	117
Vaccinites ultimus (Milovanović) H587	128	−0.08	−0.35	Min.	1402	1264	<8	<80
				Max.	2046	1522	84	798
				Mean	1703	1407	13	83
Torreites sanchezi milovanovici (Grubić) H576	68	−0.40	+0.11	Min.	1589	1132	<8	<80
				Max.	3296	1685	28	<80
				Mean	2292	1246	3	<80
Torreites sanchezi milovanovici (Grubić) H579	49	−0.45	−0.13	Min.	2390	1251	<8	<80
				Max.	4312	1616	<8	<80
				Mean	3208	1429	<8	<80
Durania aff. *mutabilis* (Stoliczka) R879	19	+0.76	+0.26	Min.	1452	410	217	936
				Max.	4147	988	508	1991
				Mean	2584	741	401	1389
Vaccinites macgillavryi (Palmer) H575	76	+0.57	+0.77	Min.	2490	314	<8	<80
				Max.	4053	1166	240	2069
				Mean	3281	721	85	661

macgillavryi, *V. grossouvrei* and in most samples of *Durania aff. mutabilis*; the latter is a radiolitid rudist with an outer shell layer that is characteristically composed of an originally hollow structure of honeycomb-like cells. These cells are now filled with diagenetic calcite so that the composition represents a mixture of original LMC and diagenetic calcite.

The data compiled on the elemental composition of modern bivalves (Fig. 4) is based on analyses of whole shells. Relatively few studies of intra-shell variations in extant and fossil shells are available, and metabolic processes which control the incorporation of minor and trace elements in bivalve shells are still insufficiently known (e.g. Rosenberg and Hughes 1991; Klein et al. 1996b). Therefore, Mn and Sr contents of individual growth bands most likely fall out of the range indicated in Fig. 4. Data regarding ontogenetic variations of Mn and Fe in modern bivalve shells are particularly scarce. Qualitative investigations yielded variable Mn concentrations in successive growth layers (Barbin et al. 1991) so that Mn concentrations which deviate from the average composition observed in Recent bivalves must not be indicative of diagenetic alterations alone, but could be the result of original ontogenetic variations. With the exception of *Durania aff. mutabilis*, Mn and Sr concentrations of the studied shells, thus, argue for a good preservation of the original LMC.

Further constraints on diagenetic alterations are provided when the elemental and isotopic compositions of shells are compared (Figs. 5, 6). Both $\delta^{13}C$ and $\delta^{18}O$ decrease with increasing Mn and Fe, and decreasing Mg and Sr in the shell of *V. macgillavryi* (Fig. 5), following expected trends that occur during meteoric

Fig. 5 Concentrations of Fe, Mn, Mg and Sr vs $\delta^{13}C$ and $\delta^{18}O$ in outer shell layer of *Vaccinites macgillavryi* from the Campanian of Somalia (H575)



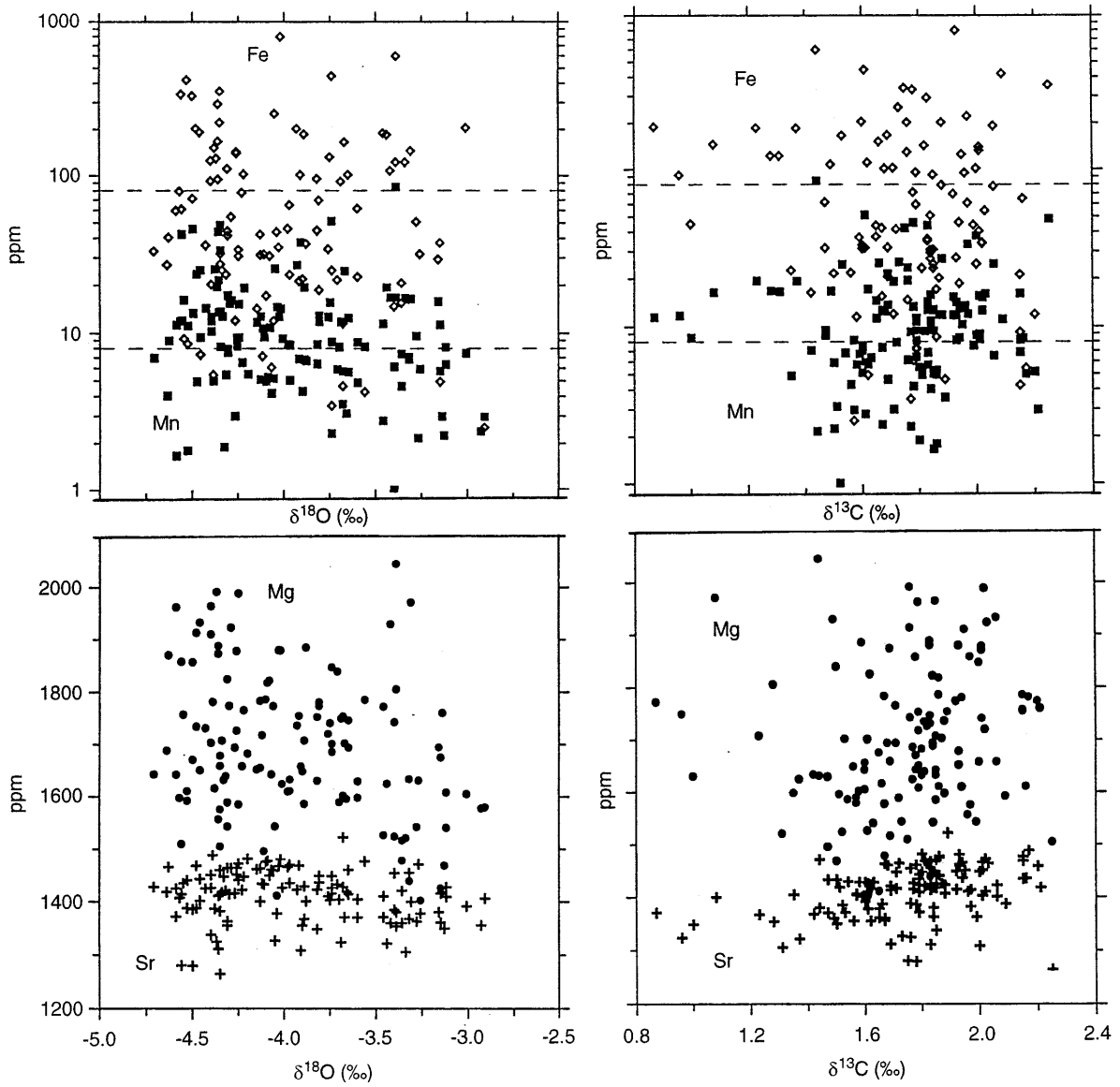


Fig. 6 Concentrations of Fe, Mn, Mg and Sr vs $\delta^{13}C$ and $\delta^{18}O$ in outer shell layer of *Vaccinites ultimus* from the Lower Campanian of northern Turkey (H587, cf. Fig. 10). *Dashed horizontal lines* indicate analytical detection limits for Fe (80 ppm) and Mn (8 ppm), respectively

diagenesis (Veizer 1983). The composition of *V. ultimus* (Fig. 6) does not indicate such diagenetic alterations, although Mn and Fe concentrations are elevated in a few samples.

The Mg and Sr concentrations of most shells cluster around the mean composition of Recent biotic calcite (Fig. 7), whereas compositions of *Vaccinites macgillavryi*, *V. grossouvrei* and *Durania* aff. *mutabilis* plot halfway towards the regression line for abiotically precipitated calcite. A diagenetic overprint of the shells of *V. macgillavryi* and *Durania* aff. *mutabilis* has been noted by comparison of chemical and isotopic compositions (Figs. 4, 5). The Mg/Sr ratio of *V. grossouvrei* also shows a pronounced offset from the regression line for modern biotic calcite. Mn and Fe are not suspiciously elevated in this specimen (Table 2) so that only low Sr concentrations indicate diagenetic alteration.

Investigations of Palaeozoic brachiopod shells have demonstrated that the preservation of original microstructures must not preclude diagenetic alteration of the isotopic composition (Rush and Chafetz 1990). Therefore, only a combination of microscopic and geochemical methods allows for a safe assessment of the preservation of the studied shells. In view of the imperfect knowledge of intra-shell variations of critical diagenetic tracer elements, such as Fe and Mn in modern bivalves, Mg–Sr ratios are considered to be most indicative of diagenetic alteration in the studied rudist shells (Fig. 7).

The following evaluations refer only to best preserved shells, i.e. those for which the retention of the original isotopic and chemical compositions

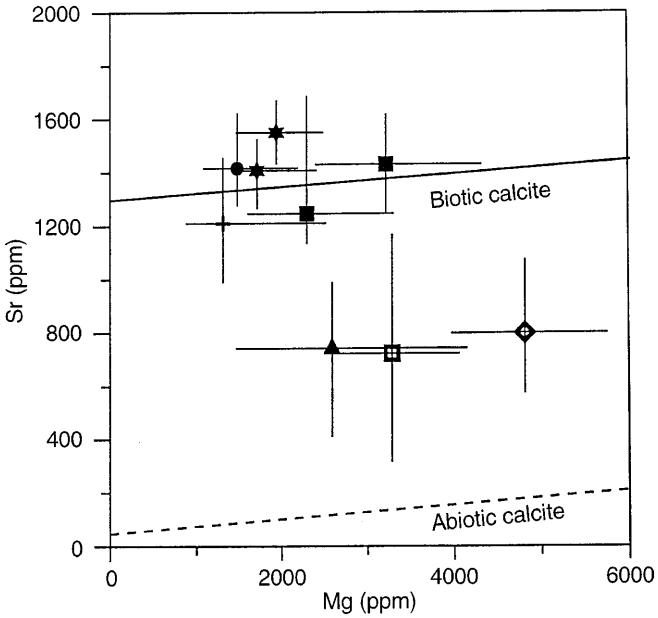


Fig. 7 Means and ranges of Mg and Sr compositions of rudist shells compared with mean compositions of modern biotically (*solid line*) and abiotically (*broken line*) precipitated calcite (Carpenter and Lohmann 1992). Symbols as in Fig. 4

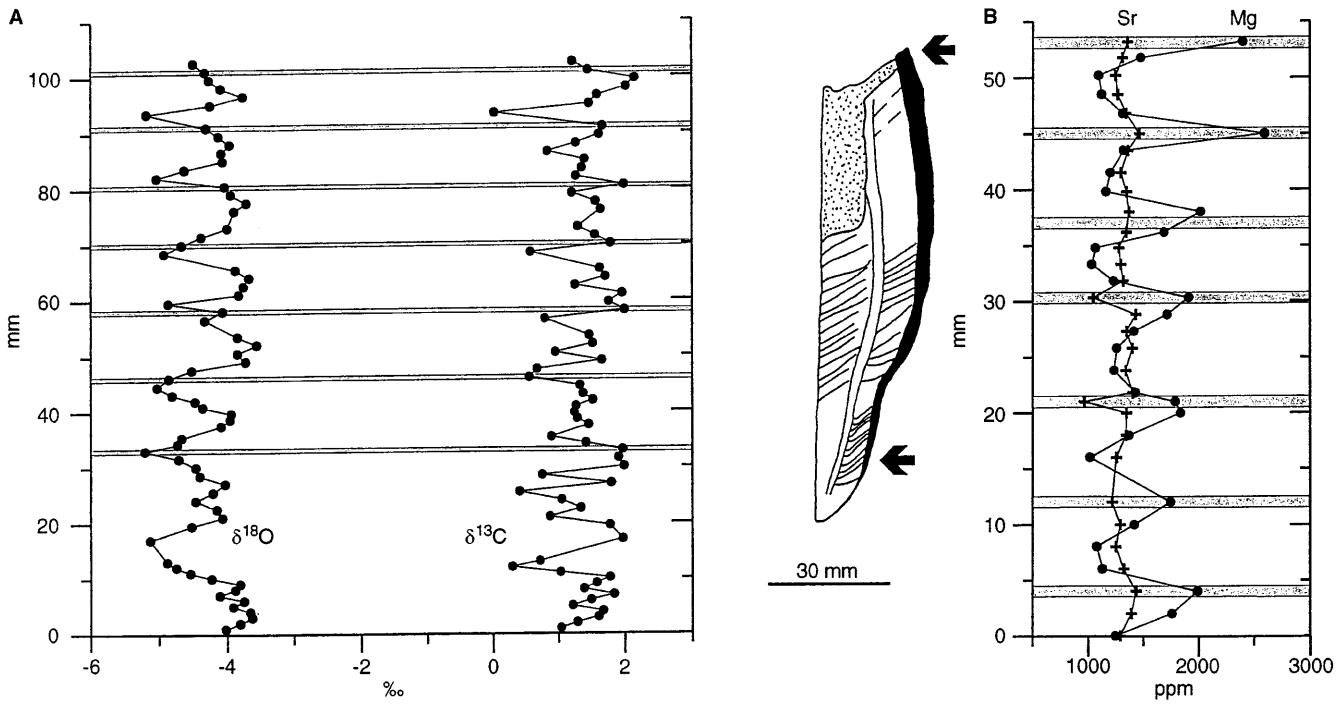
Fig. 8 Carbon and oxygen isotopic compositions along **A** anterior shell, and **B** Sr and Mg concentrations along posterodorsal shell of *Vaccinites cornuvaccinum* (H525) from the Santonian–Lower Campanian of central Greece. *Arrows* along *inset* (anterior longitudinal section) indicate sampled part of shell ($\delta^{13}C$, $\delta^{18}O$), *shaded horizontal lines* indicate dark-coloured growth lines

appears to be reasonably well constrained. The Mg and Sr concentrations of these shells cluster around the regression line for modern biotic calcite (Fig. 7).

Intra-shell variations in isotopic compositions

Analytical results of carbon and oxygen isotopic compositions are summarized in Table 1. Cyclic variations in $\delta^{18}O$ and/or $\delta^{13}C$ have been found in all shells that are considered well preserved (Figs. 8–14; see also Steuber 1996a, 1996b, 1997; Steuber et al. 1998). In less well-preserved specimens, such cycles are absent or only present in distinct parts of the shells; they have been obliterated by diagenetic repartitioning which is evident in the chemical compositions. In well-preserved specimens, isotopic cycles correspond to dark growth bands, distinct growth rugae or lamellae of the sculpture, although minima or maxima of isotopic cycles not always exactly match such structural elements (Figs. 8, 12–14). In shells of *Vaccinites ultimus* (Figs. 10, 11) no distinct dark growth bands are developed, but growth increments with low $\delta^{18}O$ are generally more dark-coloured when compared with increments with high $\delta^{18}O$. With the exception of *Torreites* (Figs. 12–14), cycles of $\delta^{18}O$ are interpreted to reflect predominantly seasonal variations in palaeotemperature. Although the retention of original $\delta^{18}O$ was not assessed in all shells from Greece and Turkey by sclerochronological analyses of elemental compositions, the presence of distinct cyclic variations within almost identical ranges of $\delta^{18}O$ is considered to prove their good preservation.

Cycles in $\delta^{13}C$ could delineate shifts in $\delta^{13}C$ of marine dissolved inorganic carbon as a result of



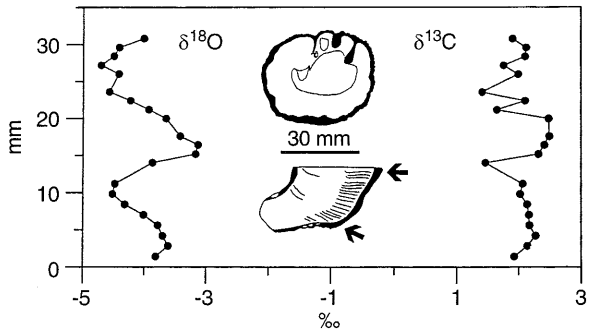


Fig. 9 Carbon and oxygen isotopic compositions of juvenile specimen of *Vaccinites cornuvaccinum* (H102) from the Santonian–Lower Campanian of central Greece. *Upper inset* shows transverse section, and *lower inset* longitudinal section of shell. *Arrows* indicate sampled part of shell

seasonal variations in marine productivity, seasonal changes in metabolic activity of the mollusks, or a combination of both. The carbon isotopic fractionation between dissolved bicarbonate and $CaCO_3$ is apparently not temperature dependent in the range of normal surface temperatures (Romanek et al. 1992), but temperature most likely controlled both metabolic activity of the rudists and marine primary production. There are weak positive correlations of $\delta^{13}C$ and $\delta^{18}O$ in the shells of *Vaccinites cornuvaccinum* and *Gorjanovicia* cf. *costata* from Greece (Table 1), and negative correlations in *V. ultimus* from northern Turkey. More significant positive correlations occur in *Torreites* and are discussed herein.

Intra-shell variations in elemental compositions

Chemical compositions have been analysed in sclerochronological profiles of nine shells (Table 2). In best-

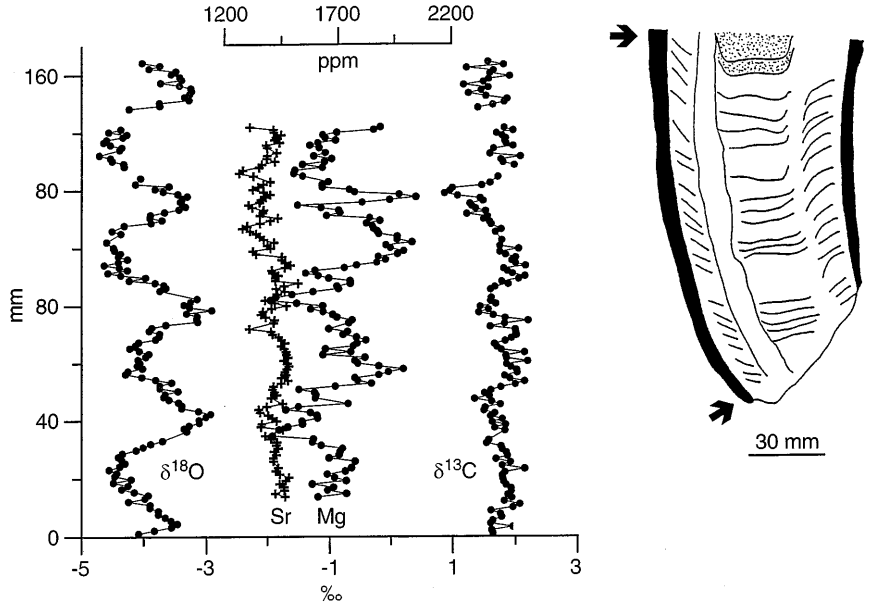


Fig. 10 Carbon and oxygen isotopic compositions, as well as Sr and Mg concentrations, in sclerochronological profile of shell of *Vaccinites ultimus* (H587) from the Lower Campanian of Amasya (northern Turkey). *Inset* shows longitudinal section and *arrows* indicate sampled part of shell

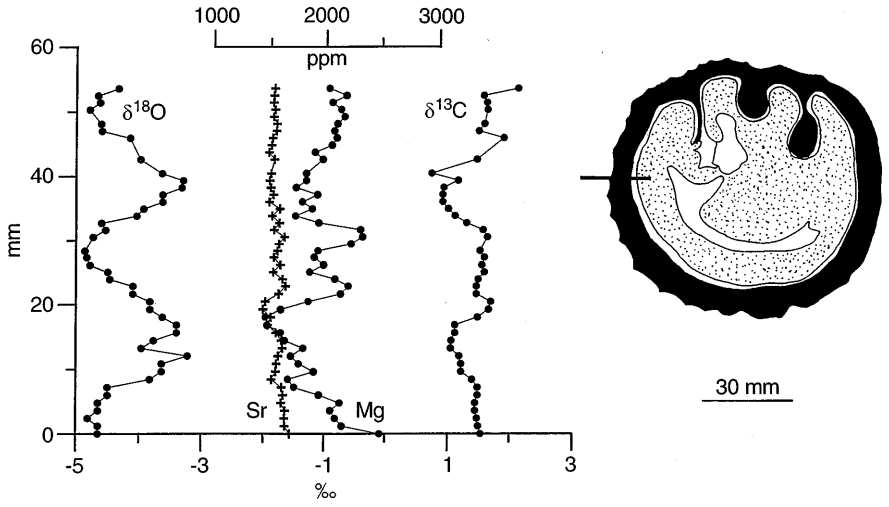


Fig. 11 Carbon and oxygen isotopic compositions, as well as Sr and Mg concentrations, in sclerochronological profile of shell of *Vaccinites ultimus* (H589) from the Lower Campanian of Amasya (northern Turkey). *Inset* shows transverse section, position of longitudinal profile is indicated by *bold line*. A more detailed figure of the isotopic composition in three profiles through different segments of the shell is given by Steuber (1996a)

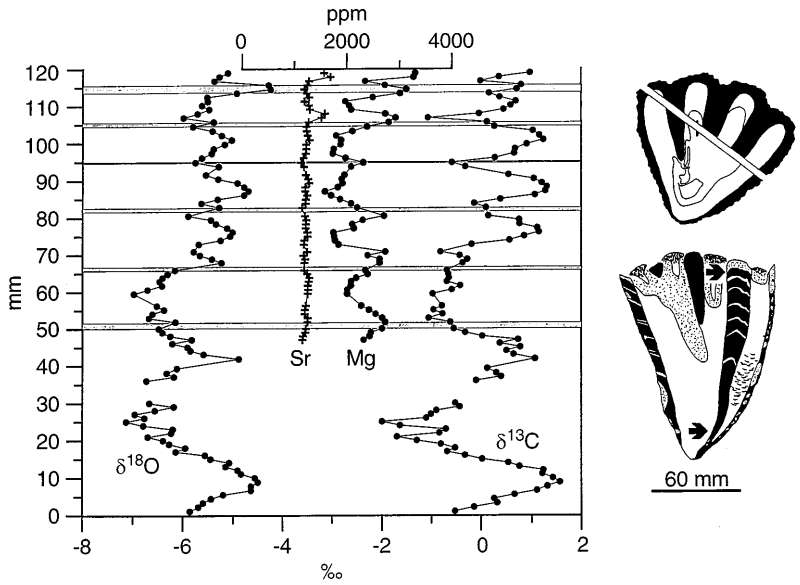


Fig. 12 Carbon and oxygen isotopic compositions, as well as Sr and Mg concentrations, in sclerochronological profile of shell of *Torreites sanchezi milovanovici* (H576) from the Lower Campanian of Oman. *Upper inset* shows transverse section, and *lower inset* longitudinal section. *Arrows* delimit sampled part of shell, *shaded horizontal lines* indicate dark-coloured growth lines (see Fig. 3)

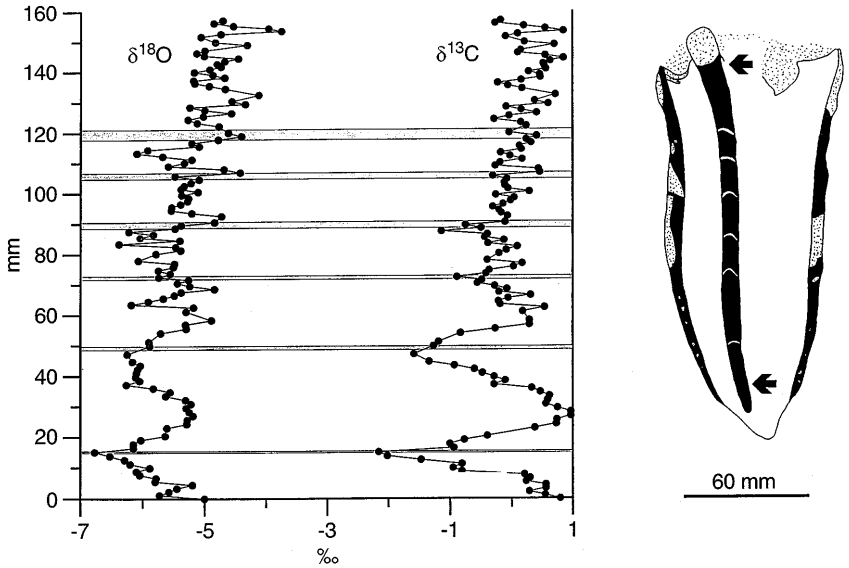


Fig. 13 Carbon and oxygen isotopic compositions in sclerochronological profile of shell of *Torreites sanchezi milovanovici* (H585) from the Lower Campanian of Oman. *Arrows along inset* (longitudinal section) delimit sampled part of shell, *shaded horizontal lines* indicate dark-coloured growth lines

preserved shells (except for *Torreites*), the concentrations of Mg are inversely correlated with $\delta^{18}O$ (Figs. 8, 10, 11; Table 2), although correlation coefficients are low for some shells and higher-order cycles are noted in two specimens of *Vaccinites ultimus* (Figs. 10, 11). The concentrations of Sr show little variations, except for an age trend of decreasing Sr in two shells of *V. ultimus* (Figs. 10, 11). Suspiciously elevated concentrations of Sr occur in two layers *of Torreites sanchezi milovanovici* (Fig. 12). Lower than average Sr concentrations in two dark growth bands of *V. cornuvaccinum* (Fig. 8B) suggest diagenetic repartitioning which is also evident in a poor preservation of shells structures of these thin layers (Steuber 1996b). The concentrations of Fe and Mn are frequently below the analytical detection limit of 80 and 8 ppm, respectively, in accordance with low concentrations that are known from the shells of modern bivalves. Consequently, Fe and Mn are herein referred to only as indicating diagenetic alterations, and no information about environmentally or biologically controlled variations can be expected.

Discussion

Intra-shell variations in Mg and Sr concentrations

Variations in the concentrations of Mg and Sr in fossil and extant marine skeletal carbonates have been related to growth rate, metabolic activity, temperature, salinity and other physical or biological parameters (e.g. Eisma et al. 1976; Lorens and Bender 1980; Rosenberg and Hughes 1991; Carpenter and Lohmann 1992; Klein et al. 1996a, 1996b). Morse and Bender (1990) critically discussed partition coefficients of Mg and Sr in calcite and concluded that a large number of

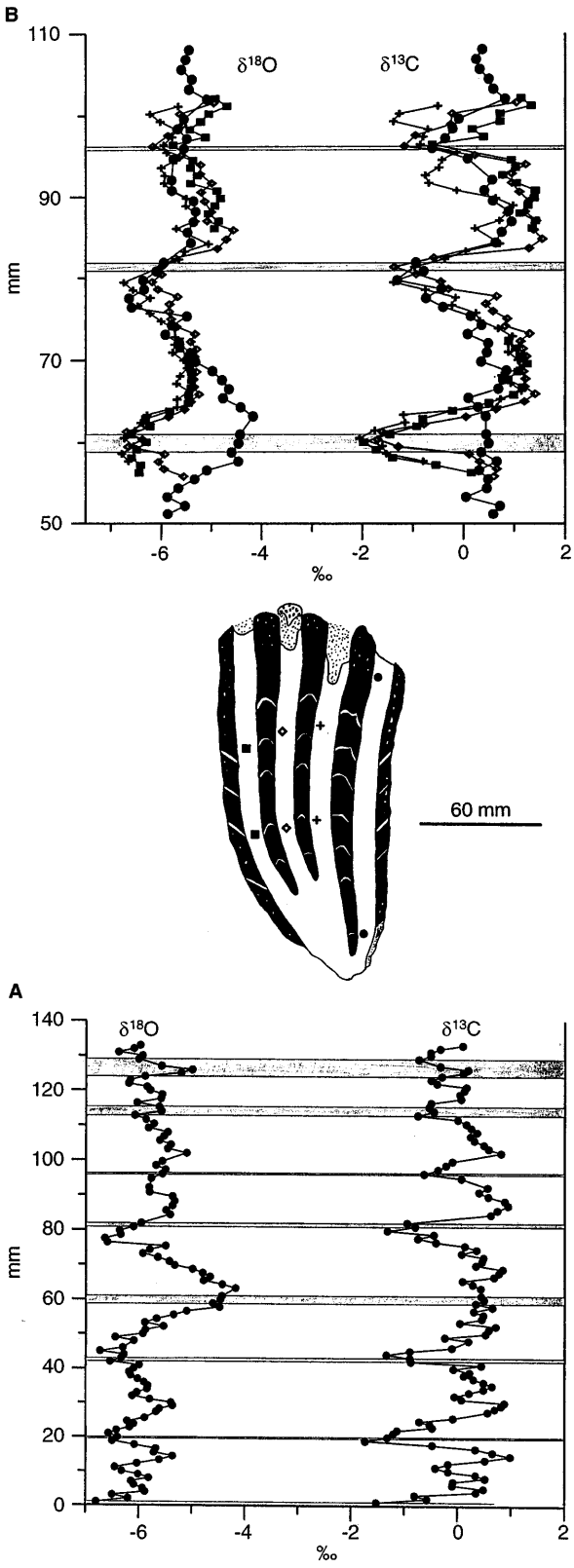


Fig. 14A,B Carbon and oxygen isotopic compositions in sclerochronological profiles of anterior pillar (*dots*), middle pillar (*crosses*), posterior pillar (*diamonds*) and posterior shell (*boxes*) of *Torreites sanchezi milovanovici* (H579) from the Lower Campanian of Oman. Part of the profile along the anterior pillar shown in **A** is compared with isotopic compositions of time-equivalent growth increments in the middle and posterior pillar, and the posterior shell in **B**. Sampled parts of the shell are indicated in *inset* (longitudinal section) by the same symbols as used in **A** and **B**. *Shaded horizontal lines* indicate dark-coloured growth lines

processes can affect the distribution of elements in calcite, and that experimental conditions certainly do not account for variations observed in nature; therefore, caution is due when applying such partition coefficients to the interpretation of the composition of natural carbonates.

Generally, biogenic calcite is not in chemical equilibrium with seawater, and inorganic partition coefficients for inorganic calcite fail to predict the chemical composition of shell carbonates. The growth of LMC shells involves biological discrimination against seawater Mg by the mollusk mantle. This has been proven by low Mg/Na ratios when compared with seawater in the extrapallial fluid of *Mytilus* (Lorens and Bender 1980). Normal seawater Mg/Ca ratios inhibit the formation of LMC and favour the formation of high-Mg calcite or aragonite. The exclusion of Mg from precipitated calcite seems to deteriorate during periods of stress (Lorens and Bender 1980).

In a detailed study of *Mytilus edulis*, Mg concentrations in the calcite shells have been found to be positively correlated with metabolic activity of the shell-secreting mantle margin, but negatively with the rate of shell secretion (Rosenberg and Hughes 1991). Accordingly, Mg concentrations of single growth increments varied significantly along the shell margin of *Mytilus*. Rosenberg and Hughes (1991) invoked that active transport of Mg could be a means to regulate allometric shells growth, as Mg inhibits the precipitation of calcite. Because of uniform increments along the mantle margin in cylindrical shells, and the constraints due to preservation in curved specimens, this was impossible to test in the analysed rudist shells. In two shells of *Vaccinites ultimus*, a higher-order cycle is recorded invariably after the annual maximum in $\delta^{18}O$ and, thus, in early spring (Figs. 10, 11). This could be related to seasonal metabolic cycles such as periods of spawning.

The consistent, though weak, covariance of Mg contents and $\delta^{18}O$ in well-preserved rudist shells agrees with results obtained from modern bivalves, and suggests a common process that controls the partitioning of both ^{18}O and Mg. This was most likely the ambient temperature which, in addition to thermodynamic partitioning (Burton and Walter 1991), also affects metabolic activity. A thermodynamic Mg-temperature relationship alone is certainly inadequate to generally explain varying Mg concentrations in mollusk shells (e.g. Klein et al. 1996a; Klein et al. 1997).

Elevated Sr in biotic calcite when compared with abiotic calcite (Fig. 7) has been interpreted to reflect kinetic fractionations (Carpenter and Lohmann 1992).

However, the concentration of Sr is not related to rates of shell accretion in *Mytilus* (Lorens and Bender 1980; Klein et al. 1996b). Intra-shell variations in Sr have been interpreted to reflect primarily variations in metabolic activity of the mantle margin (Klein et al. 1996b). According to this model, low Sr and low $\delta^{13}C$ indicate a dominance of intracellular transport of Ca to the extrapallial fluid in specimens with high metabolic activity, whereas high Sr and high $\delta^{13}C$ occur when intercellular transport of ions dominate. Following this model (Klein et al. 1996b), age trends of decreasing Sr in two shells of *V. ultimus* (Figs. 10, 11) could be interpreted to reflect increasing metabolic activity as the organisms were aging. This is supported by the observation that $\delta^{13}C$ shows similar, though less obvious, age trends in these shells. However, if metabolic activity were the major factor that controls incorporation of both Mg and Sr into the shells (Rosenberg and Hughes 1991; Klein et al. 1996b), a negative covariance between these elements would be expected. This is not the case, but could have been masked by the effect of temperature on the incorporation of Mg (Burton and Walter 1991). Further interpretation of Sr concentrations in the analysed rudist shells is difficult in the absence of significant variations and the lack of correlation with $\delta^{13}C$, $\delta^{18}O$ or Mg.

Isotopic equilibrium and vital fractionations

In contrast to most other marine invertebrates, extant bivalves appear to be the most faithful recorders of environmental conditions in their shells (Wefer and Berger 1991), because precipitation of calcite or aragonite in, or at least near to, oxygen isotopic equilibrium has been demonstrated for numerous taxonomic groups (e.g. Mook 1971; Killingley and Berger 1979; Jones et al. 1983; Pätzold et al. 1991; Klein et al. 1996a). There are, however, exceptions to this rule (Wefer 1985; Aharon and Chappell 1986). In such cases the annual temperature variations are still correctly recorded, although a certain offset in $\delta^{18}O$ occurs (Wefer and Berger 1991).

Reasonable palaeotemperatures and seasonal variations that have been found in most rudist shells imply that these Cretaceous bivalves recorded environmental conditions with similar precision and close to isotopic equilibrium. Oxygen isotopic compositions and seasonal variations are similar in all analysed shells of *Vaccinites ultimus, V. vesiculosus* and *Yvaniella alpani* from northern Turkey, as well as of *V. cornuvaccinum* and *Gorjanovicia* cf. *costata* from central Greece (Table 1). It is concluded that in these specimens the fractionation of $\delta^{18}O$ either occurred under equilibrium conditions and was independent of life habit and growth rate, or was affected by vital fractionations that caused a similar departure from isotopic equilibrium in five different species; the latter, however, is considered unlikely.

The observation that calcified inner, originally aragonitic shell layers of mid-Cretaceous rudist remains from the Gulf of Mexico have higher $\delta^{13}C$ and $\delta^{18}O$ than outer LMC layers was interpreted to indicate disequilibrium fractionation during the precipitation of the outer shell layer (Woo et al. 1992, 1993). Alternatively, this can be explained by calcitisation of aragonite in closed systems so that the original isotopic difference between aragonite and calcite (Grossmann and Ku 1986) was partially preserved (Steuber 1996b). It is, nevertheless, suspicious that $\delta^{18}O$ of rudist outer shell layers was found to be consistently lower when compared with oyster shells from the Cretaceous Gulf of Mexico (Woo et al. 1992, 1993). This may result from different habitats preferred by one group or the other. However, Sr, Mg and Mn concentrations of most shells studied by Woo et al. (1992, 1993) would fail the criteria for the recognition of well-preserved LMC mollusk shells employed in the present study.

Controlling factors for the distribution of carbon isotopes in shells of extant bivalves are difficult to identify, because biochemical processes of shell secretion are still incompletely known (Simkiss and Wilbur 1989; McConnaughey et al. 1997). Ontogenetic variations in $\delta^{13}C$ have been explained with the onset of sexual maturity or annual changes in nutrition (Wefer and Berger 1991), whereas annual fluctuations in $\delta^{13}C$ of dissolved marine bicarbonate were found to be recorded in the shell of *Mytilus* (Killingley and Berger 1979). Tracer experiments with radioisotopes revealed that a certain share of metabolic CO_2 is incorporated into the shells (Wheeler et al. 1975; Dillaman and Ford 1982). Therefore, $\delta^{13}C$ of extant bivalve shells is frequently too low with respect to inorganic equilibrium (Wefer and Berger 1991; McConnaughey et al. 1997). The amount of light, metabolic carbon in shell carbonate was found to vary significantly not only among different shells of *Mytilus* that shared the same environment, but also within time-equivalent growth increments of single shells. This has been interpreted to reflect differing rates of metabolic activity both between individuals and along the mantle margin of single individuals (Klein et al. 1996b). Varying contributions of light metabolic carbon can mask variations of $\delta^{13}C$ in the ambient marine environment so that $\delta^{13}C$ of mollusk shells is difficult to interpret, and precipitation of calcite in carbon isotopic equilibrium with ambient seawater cannot be expected.

The pattern of isotopic variation in three specimens of *Torreites* (Figs. 12–14) is significantly different from those of other shells, for which equilibrium fractionation of oxygen isotopes is most probable. Distinct dark-coloured growth bands in the shells of *Torreites* (Fig. 3) almost generally correspond to minima of cycles in $\delta^{13}C$. Matching of growth banding and $\delta^{18}O$ cycles is less significant. The amplitudes of both carbon and oxygen isotopic cycles decrease with ontogenetic age, and there is a positive correlation of $\delta^{18}O$ and $\delta^{13}C$ in all three shells (Figs. 12, 13, 14; Table 1). In one shell

(Fig. 14A), a well developed growth band at mid-height within the profile does not correspond to a negative peak in $\delta^{13}C$ but to a maximum in $\delta^{18}O$. The corresponding growth increment was analysed in three additional profiles along the middle and posterior pillar, and along the posterior shell. The negative peak in $\delta^{13}C$ is present in these additional profiles so that the isotopic composition of the anterior pillar differs significantly from that of the rest of the shell (Fig. 14B). Consequently, there are large (3‰) intra-shell variations in $\delta^{13}C$ and $\delta^{18}O$ within time-equivalent growth increments of *Torreites*. Such differences have not been noted in a shell of *Vaccinites ultimus* that was analysed in similar detail (Steuber 1996a).

Palaeotemperatures and their variations as inferred from $\delta^{18}O$ in the shells of *Torreites* are unreasonably high (Table 1). The observed isotopic pattern could indicate an estuarine environment with a seasonal influx of meteoric waters and considerably reduced salinity. Meteoric waters are depleted in ^{18}O with respect to seawater, and their dissolved inorganic carbon is commonly equilibrated with ^{13}C-depleted CO_2 of biogenic origin (Deines et al. 1974). However, there are no indications that continental runoff significantly affected the extended late Cretaceous carbonate platform of central Oman. Instead, slightly elevated salinity has been suggested by biofacies analyses of the spectacular rudist lithosomes of the region (Schumann 1995). Also, seasonally lowered salinity would not explain the decreasing amplitudes of $\delta^{13}C$ and $\delta^{18}O$ cycles with ontogenetic age. The isotopic compositions of three shells of *Torreites* are, therefore, not compatible with equilibrium precipitation from Cretaceous seawater.

Shells of *Torreites* did not only yield the largest variations in $\delta^{13}C$ and $\delta^{18}O$, but also the most negative isotopic ratios and highest Mg concentrations (Fig. 15; Tables 1, 2). Mg and $\delta^{13}C$ show a weak negative correlation, whereas there is no distinct covariance between Mg and $\delta^{18}O$ (Table 2). Mg is actively excluded during the precipitation of LMC (Lorens and Bender 1980) and inorganic equilibrium precipitation would result in higher Mg concentrations than those generally found in rudist shells and other bivalves. Elevated Mg concentrations in shells of *Torreites* suggest that environmental stress may have resulted in the breakdown of the Mg controlling mechanism in the rudist extrapallial fluid. Such perturbations could have been coupled to high metabolic activity as indicated by low $\delta^{13}C$ in growth increments with elevated Mg. Apparently, such periods of shell secretion were also linked to a significant departure from oxygen isotopic equilibrium. It remains speculative if growth bands and cycles of $\delta^{13}C$ delineate annual growth increments in *Torreites*, but they certainly indicate cycles of metabolic activity.

Compared with the isotopic composition of four shells of *V. ultimus*, samples of *Torreites* define a distinct trend of decreasing $\delta^{13}C$ and $\delta^{18}O$ (Fig. 16) which suggests kinetic fractionations. Additionally,

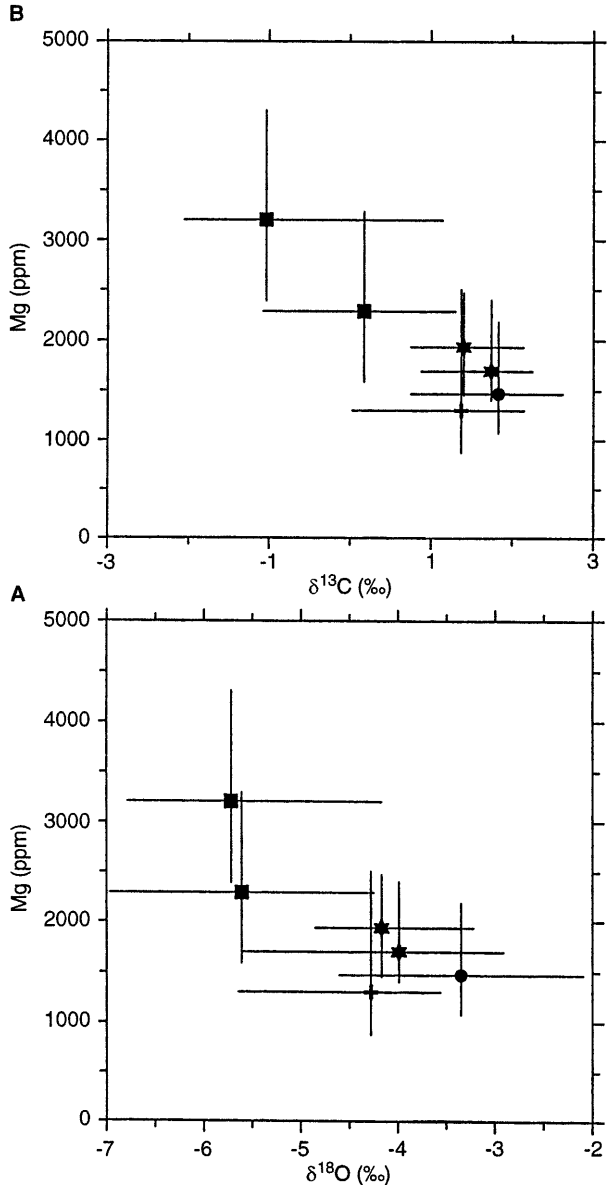


Fig. 15 Ranges and means of Mg, and **A** $\delta^{18}O$ and **B** $\delta^{13}C$ in well-preserved rudist shells. *Symbols* as in Fig. 4

amplitudes of isotopic cycles correlate with the length of the growth increment of each cycle (Fig. 17), and the average isotopic composition decreases with ontogenetic age in two shells (Figs. 12, 13). This may indicate that departure from isotopic equilibrium was related to growth rate.

Kinetic fractionations have been suggested to cause similar disequilibrium fractionations during the formation of coral skeletons (McConnaughey 1989b). Such kinetic isotope effects have been interpreted to result from disequilibrium fractionations during hydratisation and hydroxylation after diffusion of CO_2 across mineralizing membranes (McConnaughey 1989a, 1989b). Similar processes are conceivable to occur in the extrapallial fluid of mollusks. However, no rate effect on the

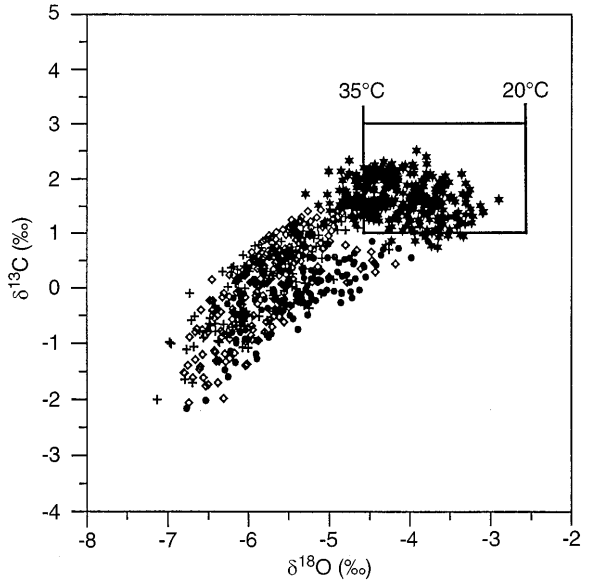


Fig. 16 Isotopic compositions of four shells of of *Vaccinites ultimus* (*stars*) and three shells of *Torreites sanchezi milovanovici* (*crosses* = H576, *diamonds* = H579, *dots* = H585), and calcite in thermodynamic equilibrium with Cretaceous seawater [–0.5‰ $\delta^{18}O$ (SMOW), 0 to +2‰ $\delta^{13}C_{HCO3-}$] in the temperature range of 20–35 °C

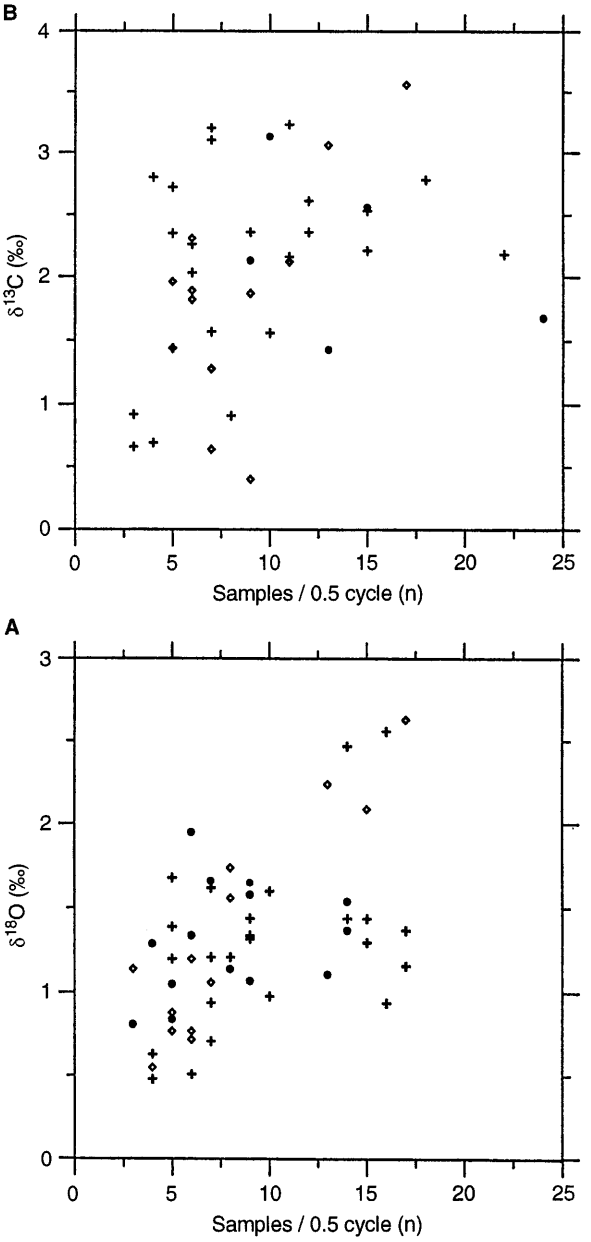


Fig. 17 Growth rate vs range of **A** $\delta^{18}O$ ($\Delta^{18}O$) and **B** $\delta^{13}C$ ($\Delta^{13}C$) in growth increments that are demarcated by dark-coloured growth bands of three shells of *Torreites sanchezi milovanovici*. Growth rate is expressed by the number of equidistantly spaced samples per growth increment to show that the correlation is not biased by insufficient resolution of cycles by low number of samples. The number of samples between turning points of isotopic cycles is indicated on the *x*-axis, resulting in two data points for each cycle. *Symbols* as in Fig. 16

carbon isotope fractionation during experimental inorganic calcite precipitation was found in the range of $10^{2.5}$ to 10^{5} $\mu mol \times m^{-2} \times h^{-1}$ (Romanek et al. 1992). These rates are higher when compared with average precipitation rates that are calculated from vertical growth increments of *Torreites*. Assuming that growth bands formed annually, precipitation rates ranged from $10^{1.97}$ $\mu mol \times m^{-2} \times h^{-1}$ in the juvenile to $10^{1.34}$ $\mu mol \times m^{-2} \times h^{-1}$ in the adult shell of the specimen shown in Fig. 12. Precipitation rates did not exceed $10^{2.1}$ $\mu mol \times m^{-2} \times h^{-1}$ in other studied rudist species. These figures, however, assume constant rates of shell accretion and do not account for seasonal or diurnal variations. Additionally, it is questionable if results from inorganic precipitation experiments can be employed to explain effects that occur during biotic precipitation of mollusk calcite.

Symbiosis with unicellular green algae modifies the isotopic composition of skeletal carbonates in most marine organisms (Erez 1977; Williams et al. 1981; McConnaughey et al. 1997). The ^{13}C content of foraminifera and corals is enhanced (Kahn and Williams 1981; Cummings and McCarty 1982), because ^{12}C is preferentially exploited for photosynthesis of the symbionts. Isotopically light CO_2 derived from the respiration of these autotrophic organisms apparently does not contribute to shell secretion. The effects of photosynthetic symbionts on the isotopic composition of bivalve shell carbonate has been investigated in the case of the extant *Tridacna* (Aharon and Chappell 1986; Jones et al. 1986; Romanek and Grossman 1989; Pätzold et al. 1991). No effect of the symbionts metabolic activity on the oxygen isotopic composition was obvious. The $\delta^{13}C$ of these shells was lower than calculated for inorganic equilibrium, but it remained unproved whether this was caused by respired CO_2 of the mollusks or of the symbionts. As the incorporation of a certain amount of ^{13}C depleted respired carbon is common in modern azooxanthellate mollusks, the

carbon isotopic composition of the shells provides no information about the presence or absence of photosymbiosis.

Morphological modifications of the left (upper) valve in several rudists and especially the characteristic pore system of the Hippuritidae have been interpreted as adaptations to the farming of photosymbionts (Philip 1972; Kauffman and Johnson 1988). The widespread occurrence of photosymbiosis in rudists is discussed controversially (Gili et al. 1995; Steuber 1997) and still lacks convincing support by analyses of the functional morphology of the group. *Torreites* is a notable exception (Skelton and Wright 1987): the characteristic pore and canal system of the Hippuritidae is absent in *Torreites*, but morphological evidence of mantle exposure strongly suggests the farming of photosymbionts, as in the extant *Tridacna*.

Linear trends of $\delta^{13}C$ and $\delta^{18}O$ that depart from isotopic equilibrium occur in the skeletons of several other groups of respiratory, non-photosymbiotic marine invertebrates, e.g. echinoids, ahermatypic corals and brachiopods (Weber and Raup 1966; McConnaughey 1989a; Carpenter and Lohmann 1995). Therefore, it is problematic to consider the large-scale deviation from isotopic equilibrium in *Torreites* (Fig. 16) as indicative of photosymbiosis. Further interpretation of the analytical data is constricted by incomplete knowledge about the physiology and biochemistry of calcification in bivalves (Simkiss and Wilbur 1989) and, in particular, about interactions between hosts and photosymbionts. Relevant interactions in hermatypic corals are also improperly understood (see reviews by Muscatine 1990; Barnes and Chalker 1990). Consequently, the geochemical results cannot resolve the problem of photosymbiosis in rudists. It is, however, suspicious that precipitation of $CaCO_3$ involved pronounced isotopic disequilibrium fractionation in a genus in which shell morphology indicates mantle exposure during life.

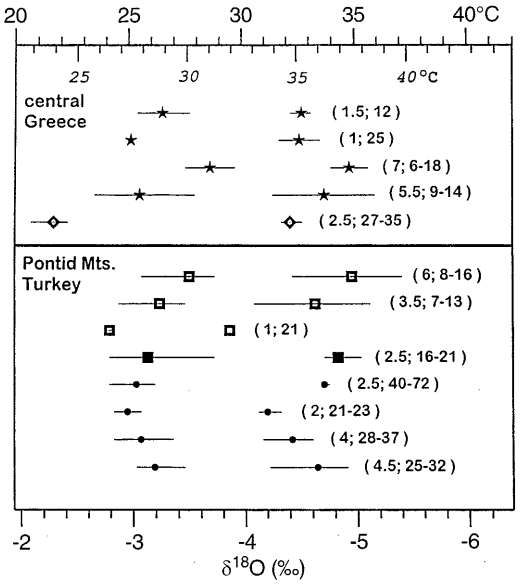


Fig. 18 Ranges and means of minima and maxima, respectively, of inferred seasonal cycles of $\delta^{18}O$. Temperature scale with inward-facing ticks calculated for –0.5‰ $\delta^{18}O_{SW}$ (SMOW), scale with outward-facing ticks for –1.0‰ $\delta^{18}O_{SW}$ (SMOW); *Vaccinites cornuvaccinum* (*stars*), *Gorjanovicia* cf. *costata* (*diamond*), *Yvaniella alpani* (*white boxes*), *V. oppeli* (*solid box*), *V. ultimus* (*dots*). *Numbers in parentheses* indicate the number of analysed $\delta^{18}O$ cycles, and minimum and maximum number of samples per cycle

Palaeoclimatic implications

As discussed previously, there is convincing evidence that environmental conditions are recorded without significant vital fractionations in shells from central Greece and northern Turkey. Mean seasonal variations in $\delta^{18}O$ are almost identical in 13 shells of five species from both localities (Fig. 18; Table 1). However, there remain some fundamental biological and geochemical constraints which complicate palaeoclimatic interpretations. The complete seasonality may not have been recorded in the shells if accretion did not occur continuously throughout the year. Prominent dark growth bands could indicate deceleration or cessation of shell growth which may occur during periods of spawning or environmental stress (Jones 1980). Unfavourable environmental conditions can even induce the dissolution of formerly secreted parts of the shell (Lutz and Rhoads 1977). Additionally, seasonal cycles may be insufficiently sampled if annual growth increments are small. Such effects can be largely excluded when minima and maxima of isotopic cycles appear well resolved and not sharply accentuated, and annual growth increments are covered with a sufficient number of samples. This is critical in shells of *V. cornuvaccinum* which show distinct growth bands that are associated with a change in shell structure and preservation (Steuber 1996b). Diagenetic repartitioning in some of these layers is indicated by low Sr concentrations (Fig. 8B). Poor preservation of these growth bands does obviously not bias the annual $\delta^{18}O$ range, as minima of cycles have been frequently noted in samples below or above such growth bands (Fig. 8A), and juvenile specimens that lack growth banding recorded similar ranges in $\delta^{18}O$ when compared with larger, adult shells (Fig. 9; Table 1). Still, complete seasonal cycles have probably not been resolved in two specimens which were sampled with less than 15 samples per cycle, although a restricted range of $\delta^{18}O$ occurs only in one of these shells (Fig. 18). Neither suspicious growth bands nor sharply accentuated extremes in isotopic cycles have been observed in shells of other studied species from Greece and Turkey, and annual growth increments have been covered by up to 72 samples (Fig. 18). Therefore, it is concluded that physical environmental conditions have been recorded without significant gaps, and that spacing of samples is gener-

ally sufficient to resolve the range of seasonal variations to a large extent.

Other constraints are due to imprecise knowledge of $\delta^{18}O$ of late Cretaceous shallow marine waters. Variation in $\delta^{18}O$ of surface waters is large in tropical marginal seas and coastal waters because influx of freshwater and evaporation potentially alter the oxygen isotopic composition of ocean water, especially in restricted environments. Evaporation and freshwater influx vary seasonally, and concomitant variations in $\delta^{18}O$ of shallow marine waters contribute to the observed range of $\delta^{18}O$ recorded in the shells. In modern oceans, highest salinity and $\delta^{18}O$ occur around 30° latitude (Zachos et al. 1994) which corresponds to the palaeogeographic setting of the Greek and Turkish localities. It is, however, questionable if this latitudinal pattern of surface water $\delta^{18}O$ can be extrapolated to the relatively narrow seaway of the late Cretaceous central Tethys (Fig. 1). Model simulations of Cretaceous ocean-atmosphere circulation also predict extended areas of elevated salinity (36.5‰) in central Tethys (Barron and Peterson 1990; Bush and Philander 1997), but salinity decreases slightly towards the central southern Eurasian continent because of its positive atmospheric moisture balance. In the eastern Mediterranean, notably in Greece, widespread Santonian-Campanian bauxites and laterites evidence a seasonally humid climate (Price et al. 1997). Therefore, significant spatial variations in salinity are conceivable for central Tethyan shallow marine waters, considering the puzzle of numerous terrains and small oceanic and epicontinental basins to the south of the Eurasian continent.

The oxygen isotopic composition of Mesozoic ocean water in the absence of large amounts of continental ice is generally estimated to be –1‰ lower than at present (Shackleton and Kennett 1975). Considering ranges in $\delta^{18}O$ and salinity of modern ocean water (Zachos et al. 1994), the average $\delta^{18}O$ of Tethyan Cretaceous ocean water is estimated within the range of –1.0 to –0.5‰ (SMOW) at 34‰ salinity ($\delta^{18}O_{SW}$). The effects of evaporation and freshwater influx on $\delta^{18}O_{SW}$ are accounted for by the following $\delta^{18}O$-salinity relationships (Fig. 19): a change in $\delta^{18}O$ of 0.18‰ per 1‰ of salinity variation due to evaporation, as found presently in the equatorial Atlantic and Sargasso Sea (Zachos et al. 1994), is adopted. This results in –0.55 to –0.05‰ (SMOW) as a plausible estimate for central Tethyan ocean water at a salinity of 36.5‰, as predicted by general circulation models (Barron and Peterson 1990; Bush and Philander 1997). Reduced meridional temperature gradients certainly reduced latitudinal $\delta^{18}O$ gradients of precipitation (Barron and Washington 1985) so that –6‰ $\delta^{18}O$ (SMOW) is estimated as the mean oxygen isotopic composition of freshwater that potentially lowered the salinity of Tethyan ocean water. Within this framework of $\delta^{18}O$–salinity relationships, the observed seasonality in $\delta^{18}O$ could be ascribed to salinity changes in the euhaline range of 30–38‰ and almost constant temperatures of 30 or

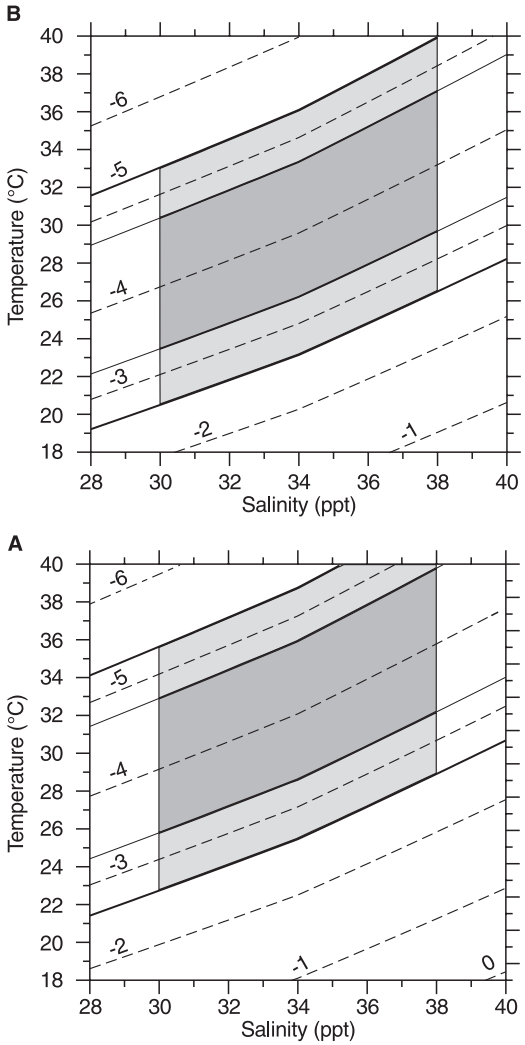


Fig. 19 Variations in $\delta^{18}O$ in relation to salinity and temperature of seawater, assuming **A** –0.5‰ $\delta^{18}O$ (SMOW) and **B** –1.0‰ $\delta^{18}O$ (SMOW) at 34‰ salinity. Relationship $\delta^{18}O$–salinity is estimated at 0.18‰ per 1‰ $\delta^{18}O$ for evaporation, and freshwater influx of –6‰ $\delta^{18}O$ (see text); *dark shade* indicates mean seasonality recorded in shells of *V. cornuvaccinum* from Greece and in rudists from Amasya, *light shade* shows seasonal extremes (see Fig. 17). Means and extremes are similar for both localities

32.5 °C at $\delta^{18}O_{SW}$ of –1.0 and –0.5‰ (SMOW), respectively (Fig. 19). Although salinity variations of this magnitude would not disagree with the normal marine biofacies at both localities, this scenario is unreasonable considering the subtropical palaeolatitude of both localities. A monsoonal climate with summerly freshwater influx would enhance annual $\delta^{18}O$ ranges, whereas increased continental runoff during winter and ^{18}O enrichment by evaporation during summer would diminish them, and cause an underestimation of annual temperature ranges if salinity changes are not considered. Palaeotemperatures and seasonality, assuming these extreme conditions in a salinity range of 30–38‰, are listed in Table 3. Mean summer temperatures amount to 40 °C when salinity increased to 38‰ during

Table 3. Palaeotemperatures and seasonality calculated for different $\delta^{18}O$ and salinity of late Cretaceous shallow marine waters for mean annual minima and maxima of $\delta^{18}O$ of *Vaccinites cornuvaccinum* from Greece and rudist shells from northern Turkey (cf. Figs. 18, 19)

Salinity (‰)		$\delta^{18}O_{SW}$	Temperature (°C)		Seasonality
Winter	Summer	(‰)	Winter	Summer	(°C)
30	38	−0.5	26	40	14
34	34	−0.5	29	36	7
36.5	36.5	−0.5	31	38	7
38	30	−0.5	32	33	1
30	38	−1.0	23	37	14
34	34	−1.0	26	33	7
36.5	36.5	−1.0	28	35	7
38	30	−1.0	29.5	30.5	1

Values adopted for $\delta^{18}O$-salinity relationships during evaporation and freshwater influx are explained in the text

summer and $\delta^{18}O_{SW}$ was –0.5‰ (SMOW). Coolest temperatures of 23 °C are obtained when salinity was 30‰ in winter and $\delta^{18}O_{SW}$ was –1.0‰ (SMOW). Seasonality amounts to 14 °C when evaporation during summer and freshwater influx during winter had a maximum contribution to $\delta^{18}O$ of the shells. Seasonality was 7 °C, if salinity was constant during the year and $\delta^{18}O$ is related to temperature only.

Reduced salinity may be recognized by low $\delta^{13}C$ of shell carbonates, as freshwater bicarbonate is generally equilibrated with a phytogenic CO_2 source (Deines et al. 1974). Mixing of freshwater (–15‰ $\delta^{13}C$) and marine water (0‰ $\delta^{13}C$) that results in a salinity of 30‰ would lower $\delta^{13}C$ of the mixed fluid by 1.8‰. In fact, a weak positive correlation of $\delta^{13}C$ and $\delta^{18}O$ is noted in shells of *V. cornuvaccinum* from Greece (Table 1), but this could also be due to seasonally varying rates in metabolic activity or other factors that determine the carbon isotopic composition of marine inorganic carbon, as discussed previously. Evaporation in the considered magnitude does not significantly alter $\delta^{13}C$ of marine waters (Stiller et al. 1985); therefore, as no other proxies for palaeosalinity and $\delta^{18}O$ are available for the range that is relevant for the present study, seasonal temperature and salinity variations cannot be separated more precisely.

A comparison of the environmental settings of the two rudist associations may provide some further indications on possible salinity variations. In Greece, *V. cornuvaccinum* thrived in protected, and probably restricted, lagoonal environment where salinity most probably varied seasonally. Suspiciously, maximum $\delta^{18}O$ of *Gorjanovicia* cf. *costata* is consistently higher in 2.5 cycles than that of four shells of *Vaccinites cornuvaccinum*. *G.* cf. *costata* lived on the seaward slope of an offshore rudist bank and was probably less affected by salinity changes and, thus, gives a better estimate of open-ocean temperatures (Fig. 18). Lower $\delta^{18}O$ in *V. cornuvaccinum* during the cool season could reflect freshwater influx into its lagoonal habitat. Seasonal variations of salinity were probably of minor importance at the Turkish locality, where the studied rudists and associated colonial corals lived on a calcareous-siliciclastic ramp without indications of restriction (Steuber et al. 1998).

The oxygen isotopic composition of oyster and rudist shells from the mid-Cretaceous of the Gulf of Mexico was found to be significantly higher when compared with the data presented here and has been interpreted to reflect high salinity of surface waters (Woo et al. 1992, 1993). An evaluation of the temperature ranges obtained by assuming various $\delta^{18}O$–salinity relationships for the eastern Mediterranean rudists suggests that salinity in their habitat did not exceed 35–36‰. Minima in $\delta^{18}O$ of shells from both localities would translate to temperatures in excess of 40 °C if $\delta^{18}O_{SW}$ was –0.5‰ (SMOW) and salinity was higher than 35‰. Such temperatures were most probably not tolerated by bivalves.

Despite the discussed potential for errors in the calculation of palaeotemperatures, it is evident that shallow marine waters of the late Cretaceous Tethys were at least as warm as ocean water at present comparable latitudes. This agrees with mean equatorial palaeotemperatures of 27–32 °C reported from magnesian calcite and aragonitic rudist remains from Maastrichtian platform carbonates of a Pacific guyot (Wilson and Opdyke 1996), as well as with predictions of Cretaceous climate from general circulation models (Barron et al. 1995; Bush and Philander 1997; Hay et al. 1997). Extremely warm surface waters from the Turonian through the early Campanian of the southern high latitudes are evident in $\delta^{18}O$ of planktonic foraminifera (Huber et al. 1995). Cool Cenomanian palaeotemperatures at low to intermediate latitudes determined from the isotopic composition of planktonic foraminifera (Sellwood et al. 1994) increase by approximately 2.3 C, when an appropriate salinity correction is used (Zachos 1994) and, then, are similar to modern sea-surface temperatures.

Conclusion

In well-preserved shells of rudist bivalves, cycles of $\delta^{18}O$ are interpreted to reflect seasonal variations in temperature and/or salinity. Large-scale disequilibrium fractionations of carbon and oxygen isotopes have been identified in shells of *Torreites*, and are linked to elevated Mg concentrations. This suggests that isotopic disequilibrium in *Torreites* is related to a failure of biochemical processes that are also responsible for the exclusion of Mg from LMC of the outer shell layer. Although morphological evidence indicates mantle exposure in *Torreites*, disequilibrium fractionation of ^{13}C and ^{18}O must not be a consequence of photosymbiosis. Similar linear trends of $\delta^{13}C$ and $\delta^{18}O$ occur also in other groups of non-photosymbiotic organisms, but not in the extant, photosymbiotic *Tridacna*. Impor-

tantly, large-scale disequilibrium fractionations similar to those observed in *Torreites* are unknown in extant bivalves. This highlights the problem of vital effects in palaeoclimatic interpretations of isotopic proxies, also in groups of organisms for which isotopic fractionations have been constrained by studies of modern representatives. Vital effects could also have affected the isotopic composition of the other studied rudist species. If small, they may result in inconspicuous shifts of the isotopic compositions that are difficult to detect but can severely disturb palaeoclimatic interpretations. Such constraints are minimized when several species from associations that are preserved in life position yield similar means and ranges of annual $\delta^{18}O$ cycles. This is the case for 13 specimens of five rudist species studied from two localities in central Greece and northern Turkey. They are considered as reliable recorders of the temperature and salinity of late Cretaceous central Tethyan surface waters.

A large potential for errors in the calculation of palaeotemperatures is due to imprecise knowledge of the $\delta^{18}O$–salinity relationship of Cretaceous seawater in the absence of independent proxies for these parameters. The isotopic data indicate that salinity could not have been considerably higher than 34–36.5‰, as this would result in summer temperatures in excess of 40 °C. A seasonality of 7 °C is calculated if constant salinity throughout the year is assumed. Elevated salinity in summer due to evaporation and/or fresh water influx during winter would enhance the seasonal temperature range. Mean seasonal extremes are within the range of 26–38 °C, if boundary conditions of 36.5 and 34‰ salinity, and –0.5 and –1.0‰ $\delta^{18}O_{SW}$ (SMOW), respectively, are considered (Table 3). These results agree with global circulation models which predict tropical and subtropical late Cretaceous sea-surface temperatures that were higher than at present.

Acknowledgements I thank J.H. Schroeder, D. Schumann and P. Skelton for the donation of rudist specimens, and A. Hemman and M. Joachimski for some of the isotopic analyses. Comments by M. Joachimski on a previous version of the manuscript and reviews by P.K. Swart and W.-C. Dullo are gratefully acknowledged. This study was funded by Deutsche Forschungsgemeinschaft (Ste 670/2, Ste 670/3).

References

Aharon P, Chappell J (1986) Oxygen isotopes, sea level changes and the temperature history of a coral reef environment in New Guinea over the last 105 years. Palaeogeogr Palaeoclimatol Palaeoecol 56:337–379

Al-Aasm IS, Veizer J (1982) Chemical stabilization of low-Mg calcite: an example of brachiopods. J Sediment Petrol 52:1101–1109

Al-Aasm IS, Veizer J (1986a) Diagenetic stabilization of aragonite and low-Mg calcite, I. Trace elements in rudists. J Sediment Petrol 56:138–152

Al-Aasm IS, Veizer J (1986b) Diagenetic stabilization of aragonite and low-Mg calcite. II. Stable isotopes in rudists. J Sediment Petrol 56:763–770

Anderson TF, Arthur MA (1983) Stable isotopes of oxygen and carbon and their application to sedimentologic and paleoenvironmental problems. SEPM Short Course 10:1–151

Banner JL, Hanson GN (1990) Calculation of simultaneous isotopic and trace element variations during water–rock interaction with application to carbonate diagenesis. Geochim Cosmochim Acta 54:3123–3137

Barbin V, Ramseyer K, Debenay JP, Schein E, Roux M, Decrouez D (1991) Cathodoluminiscence of recent biogenic carbonates: an environmental and ontogenetic fingerprint. Geol Mag 128:19–26

Barnes DJ, Chalker BE (1990) Calcification and photosynthesis in reef-building corals and algae. In: Dubinsky Z (ed) Coral reefs. Elsevier, Amsterdam, pp 109–131

Barron EJ, Peterson WH (1990) Mid-Cretaceous ocean circulation: results from model sensitivity studies. Paleoceanography 5:319–337

Barron EJ, Washington WM (1985) Warm Cretaceous climates: high atmospheric CO_2 as a plausible mechanism. In: Sundquist ET, Broecker WS (eds) The carbon cycle and atmospheric CO_2: natural variations Archean to Present. Geophys Monogr 32:546–553

Barron EJ, Fawcett PJ, Peterson WH, Pollard D, Thompson SL (1995) A "simulation" of mid-Cretaceous climate. Paleoceanography 10:953–962

Brand U, Veizer J (1980) Chemical diagenesis of a multicomponent carbonate system. 1. Trace elements. J Sediment Petrol 50:1219–1236

Burton EA, Walter LM (1991) The effects of pCO_2 and temperature on magnesium incorporation in calcite in seawater and $MgCl_2$–$CaCl_2$ solutions. Geochim Cosmochim Acta 55:777–785

Bush ABG, Philander SGH (1997) The late Cretaceous: simulation with a coupled atmosphere–ocean general circulation model. Paleoceanography 12:495–516

Carpenter SJ, Lohmann KC (1992) Sr/Mg ratios of modern marine calcite: empirical indicators of ocean chemistry and precipitation rate. Geochim Cosmochim Acta 56:1837–1849

Carpenter SJ, Lohmann KC (1995) $\delta^{18}O$ and $\delta^{13}C$ values of modern brachiopod shells. Geochim Cosmochim Acta 59:3749–3764

Cummings CE, McCarty HB (1982) Stable carbon isotope ratios in *Astrangia danae*: evidence for algal modification of carbon pools used in calcification. Geochim Cosmochim Acta 46:1125–1129

Deines P, Langmuir D, Harmon RS (1974) Stable carbon isotope ratios and the existence of a gas phase in the evolution of carbonate ground waters. Geochim Cosmochim Acta 38:1147–1164

Dercourt J, Zonenshain LP, Ricou LE, Kazmin VE, Le Pichon X, Knipper AL, Grandjacquet C, Sborshchikov IM, Boulin J, Sorokhtin O, Geyssant J, Lepvrier C, Biju-Duval B, Sibuet J-C, Savostin LA, Westphal M, Lauer J-P (1985) Présentation de 9 cartes paléogéographiques au 1/20.000.000 s'étendant de l'Atlantique au Pamir pour la période du Lias à l'actuel. Bull Soc Géol France 1:637–652

Dillaman RM, Ford SE (1982) Measurement of calcium carbonate deposition in molluscs by controlled etching of radioactively labeled shells. Mar Biol 66:133–143

Eisma D, Mook WG, Das HA (1976) Shell characteristics, isotopic composition and trace element contents of some euryhaline molluscs as indicators of salinity. Palaeogeogr Palaeoclimatol Palaeoecol 19:39–62

Erez J (1977) Influence of symbiotic algae on the stable isotope composition of hermatypic corals: a radioactive tracer approach. Proc 3rd Int Coral Reef Symp, pp 563–569

Gili E, Masse J-P, Skelton PW (1995) Rudists as gregarious sediment-dwellers, not reef-builders, on Cretaceous carbonate platforms. Palaeogeogr Palaeoclimatol Palaeoecol 118:245–267

Grossman EL, Ku T-L (1986) Oxygen and carbon isotope fractionation in biogenic aragonite: temperature effects. Chem Geol 59:59–74

Hallam A, Price NB (1968) Environmental and biochemical control of strontium in shells of *Cardium edule*. Geochim Cosmochim Acta 32:319–328

Hay WW, DeConto RM, Wold CN (1997) Climate: Is the past the key to the future? Geol Rundsch 86:471–491

Huber BT, Hodell DA, Hamilton CP (1995) Middle-late Cretaceous climate of the southern high latitudes: stable isotope evidence of minimal equator-to-pole thermal gradients. Geol Soc Am Bull 107:1164–1191

Jones DS (1980) Annual cycle of shell growth increment formation in two continental shelf bivalves and its paleoecologic significance. Paleobiology 6:331–340

Jones DS, Williams DF, Arthur MA (1983) Growth history and ecology of the atlantic surf clam, *Spisula solidissima* (Dillwyn), as revealed by stable isotopes and annual shell increments. J Exp Mar Biol Ecol 73:225–242

Jones DS, Williams DF, Arthur MA, Krantz DE (1984) Interpreting the paleoenvironmental, paleoclimatic and life history records in mollusc shells. Géobios Mém Spéc 8:333–339

Jones DS, Williams DF, Romanek CS (1986) Life history of symbiont bearing giant clams from stable isotope profiles. Science 231:46–48

Kahn MI, Williams DF (1981) Oxygen and carbon isotopic composition of living planktonic foraminifera from the Northeast Pacific Ocean. Palaeogeogr Palaeoclimatol Palaeoecol 33:47–69

Kauffman EG, Johnson CC (1988) The morphological and ecological evolution of middle and Upper Cretaceous reef-building rudists. Palaios 3:194–216

Kennedy WJ, Taylor JD (1968) Aragonite in rudists. Proc Geol Soc Lond 1645:325–331

Killingley JS, Berger WH (1979) Stable isotopes in a mollusk shell: detection of upwelling events. Science 205:186–188

Klein RT, Lohmann KC, Thayer CW (1996a) Bivalve skeletons record sea-surface temperature and $\delta^{18}O$ via Mg/Ca and $^{18}O/^{16}O$ ratios. Geology 24:415–418

Klein RT, Lohmann KC, Thayer CW (1996b) Sr/Ca and $^{13}C/^{12}C$ ratios in skeletal calcite of *Mytilus trossulus*: covariation with metabolic rate, salinity, and carbon isotopic composition of seawater. Geochim Cosmochim Acta 60:4207–4221

Klein RT, Lohmann KC, Kennedy GL (1997) Elemental and isotopic proxies of paleotemperature and paleosalinity: climate reconstruction of the marginal northeast Pacific ca. 80 ka. Geology 25:363–366

Leutwein F, Waskowiak R (1962) Geochemische Untersuchungen an rezenten Molluskenschalen. N Jahrb Mineral Abhandl 99:45–78

Lorens RB, Bender ML (1980) The impact of solution chemistry on *Mytilus edulis* calcite and aragonite. Geochim Cosmochim Acta 44:1265–1278

Lutz RA, Rhoads DC (1977) Anaerobiosis and a theory of growth line formation. Science 198:1222–1227

McConnaughey T (1989a) ^{13}C and ^{18}O disequilibrium in biological carbonates. I. Patterns. Geochim Cosmochim Acta 53:151–162

McConnaughey T (1989b) ^{13}C and ^{18}O disequilibrium in biological carbonates. II. In vitro simulation of kinetic isotope effects. Geochim Cosmochim Acta 53:163–171

McConnaughey T, Burdett J, Whelan JF, Paull CK (1997) Carbon isotopes in biological carbonates: respiration and photosynthesis. Geochim Cosmochim Acta 61:611–622

Milliman JD (1974) Marine carbonates. Springer, Berlin Heidelberg New York, pp 1–375

Mook WG (1971) Palaeotemperatures and chlorinities from stable carbon and oxygen isotopes in shell carbonate. Palaeogeogr Palaeoclimatol Palaeoecol 9:245–263

Morse JW, Bender ML (1990) Partition coefficients in calcite: examinations of factors influencing the validity of experimental results and their application to natural systems. Chem Geol 82:265–277

Muscatine L (1990) The role of symbiotic algae in carbon and energy flux in reef corals. In: Dubinsky Z (ed) Coral reefs. Elsevier, Amsterdam, pp 75–88

Pannella G, MacClintock C (1968) Biological and environmental rhythms reflected in molluscan shell growth. J Paleontol 42:64–81

Pätzold J, Heinrichs JP, Wolschendorf K, Wefer G (1991) Correlation of stable isotope temperature records with light attenuation profiles in reef-dwelling *Tridacna* shells. Coral Reefs 10:65–69

Philip J (1972) Paléoécologie des formations à rudistes du Crétacé supérieur: l'exemple du Sud-Est de la France. Palaeogeogr Palaeoclimatol Palaeoecol 12:205–222

Pilkey OH, Goodell HG (1963) Trace elements in recent mollusk shells. Limnol Oceanogr 8:137–148

Pons JM, Schroeder JH, Höfling R, Moussavian E (1992) Upper Cretaceous rudist assemblages in northern Somalia. Geol Romana 28:219–241

Price GD, Valdes PJ, Sellwood BW (1997) Prediction of modern bauxite occurrence: implications for climate reconstructions. Palaeogeogr Palaeoclimatol Palaeoecol 131:1–13

Rhoads DC, Lutz RA (1980) Skeletal records of environmental change. In: Rhoads DC, Lutz RA (eds) Skeletal growth of aquatic organisms. Topics Geobiol 1:1–19

Romanek CS, Grossman EL (1989) Stable isotope profiles of *Tridacna maxima* as environmental indicators. Palaios 4:402–413

Romanek CS, Grossman EL, Morse JW (1992) Carbon isotopic fractionation in synthetic aragonite and calcite: effects of temperature and precipitation rate. Geochim Cosmochim Acta 56:419–430

Rosenberg GD, Hughes WW (1991) A metabolic model for the determination of shell composition in the bivalve mollusc, *Mytilus edulis*. Lethaia 24:83–96

Ross DJ, Skelton PW (1993) Rudist formations of the Cretaceous: a palaeoecological, sedimentological and stratigraphic review. In: Wright P (ed) Sedimentology review 1. Blackwell, London, pp 73–91

Rush PF, Chafetz HS (1990) Fabric-retentive, non-luminescent brachiopods as indicators of original $\delta^{13}C$ and $\delta^{18}O$ composition: a test. J Sediment Petrol 60:968–981

Schumann D (1995) Upper Cretaceous rudist and stromatoporoid associations of central Oman (Arabian Peninsula). Facies 32:189–202

Sellwood BW, Price GD, Valdes PJ (1994) Cooler estimates of Cretaceous temperatures. Nature 370:453–455

Shackleton NJ, Kennett JP (1975) Paleotemperature history of the Cenozoic and the initiation of Antarctic glaciation: oxygen and carbon isotope analyses in DSDP sites 277, 279, and 281. Init Rep DSDP 29:743–755

Simkiss K, Wilbur KM (1989) Biomineralization: cell biology and mineral deposition. Academic Press, London, pp 1–337

Skelton PW (1974) Aragonitic shell structures in the rudist *Biradiolites* and some palaeobiological inferences. Géol Méditerran 1–2:63–74

Skelton PW, Wright VP (1987) A Caribbean rudist bivalve in Oman: island hopping across the Pacific in the late Cretaceous. Palaeontology 30:505–529

Skelton PW, Nolan SC, Scott RW (1990) The Maastrichtian transgression onto the northwestern flank of the Proto-Oman Mountains: sequences of rudist bearing beach to open shelf facies. In: Robertson AHF, Searle PM, Ries AC (eds) The geology and tectonics of the Oman region. Geol Soc Spec Publ 49:521–547

Steuber T (1996a) Stable isotope sclerochronology of rudist bivalves: growth rates and late Cretaceous seasonality. Geology 24:315–318

Steuber T (1996b) Stable isotope sclerochronology of *Vaccinites cornuvaccinum* (Hippuritidae) from Beotia (Greece). Rev Mex Ciencias Geol 12:307–314
Steuber T (1997) Hippuritid rudist bivalves in siliciclastic settings: functional adaptations, growth rates and strategies. Proc 8th Int Coral Reef Symp 2:1761–1766
Steuber T, Yilmaz C, Löser H (1998) Growth rates of early Campanian rudists in a siliciclastic-calcareous setting (Pontid Mts., North-central Turkey). Geobios Mém Spéc 22:385–401
Stiller M, Rounick JS, Shasha S (1985) Extreme carbon-isotope enrichments in evaporating brines. Nature 316:434–435
Turekian KK, Armstrong RL (1960) Magnesium, strontium, and barium concentrations and calcite–aragonite ratios of some recent molluscan shells. J Mar Res 18:133–151
Veizer J (1983) Trace elements and isotopes in sedimentary carbonates. In: Reeder RJ (ed) Carbonates: mineralogy and chemistry. Rev Mineral 11:265–299
Vinogradov AP (1953) The elementary chemical composition of marine organisms. Sears Foundation Mar Res Mem 11:1–647
Weber JN, Raup DM (1966) Fractionation of the stable isotopes of carbon and oxygen in marine organisms: the Echinoidea. Part 1. Variation of C^{13} and O^{18} content within individuals. Geochim Cosmochim Acta 30:681–703
Wefer G (1985) Die Verteilung stabiler Isotope in Kalkschalen mariner Organismen. Geol Jahrb A82:1–111
Wefer G, Berger WH (1991) Isotope paleontology: growth and composition of extant calcareous species. Mar Geol 100:207–248
Wheeler AP, Blackwelder PL, Wilbur KM (1975) Shell growth in the scallop *Argopecten irradians*. I. Isotope incorporation with reference to diurnal growth. Biol Bull 148:472–482
Williams DF, Röttger R, Schmaljohann R, Keigwin L (1981) Oxygen and carbon isotopic fractionation and algal symbiosis in the benthic foraminiferan *Heterostegina depressa*. Palaeogeogr Palaeoclimatol Palaeoecol 33:231–251
Wilson PA, Opdyke BN (1996) Equatorial sea-surface temperatures for the Maastrichtian revealed through remarkable preservation of metastable carbonate. Geology 24:555–558
Woo KS, Anderson TF, Railsback LB, Sandberg PA (1992) Oxygen isotope evidence for high salinity surface seawater in the mid-Cretaceous Gulf of Mexico: implications for warm, saline deepwater formation. Paleoceanography 7:673–685
Woo KS, Anderson TF, Sandberg PA (1993) Diagenesis of skeletal and nonskeletal components of mid-Cretaceous limestones. J Sediment Petrol 63:18–32
Zachos JC, Stott LD, Lohmann KC (1994) Evolution of early Cenozoic marine temperatures. Paleoceanography 9:353–387